CRevolution 2: Origin and Evolution of the
Colorado River System II themed issue

Importance of groundwater in propagating downward integration of the 6–5 Ma Colorado River system: Geochemistry of springs, travertines, and lacustrine carbonates of the Grand Canyon region over the past 12 Ma

L.C. Crossey[1], K.E. Karlstrom[1], R. Dorsey[2], J. Pearce[3], E. Wan[4], L.S. Beard[5], Y. Asmerom[1], V. Polyak[1], R.S. Crow[1], A. Cohen[6], J. Bright[6], and M.E. Pecha[6]

[1]*Department of Earth and Planetary Sciences, University of New Mexico, Albuquerque, New Mexico, 87131, USA*
[2]*Department of Geological Sciences, 1272 University of Oregon, Eugene, Oregon 97403-1272, USA*
[3]*U.S. Forest Service, Grand Mesa, Uncompahgre and Gunnison National Forests, Paonia Ranger District, 403 North Rio Grande Avenue, P.O. Box 1030, Paonia, Colorado 81428, USA*
[4]*U.S. Geological Survey, 345 Middlefield Road, MS977, Menlo Park, California 94025, USA*
[5]*U.S. Geological Survey, 2255 North Gemini Drive, Flagstaff, Arizona 86001, USA*
[6]*Department of Geosciences, The University of Arizona, 1040 East 4th Street, Tucson, Arizona 85721, USA*

ABSTRACT

We applied multiple geochemical tracers ($^{87}Sr/^{86}Sr$, [Sr], $\delta^{13}C$, and $\delta^{18}O$) to waters and carbonates of the lower Colorado River system to evaluate its paleohydrology over the past 12 Ma. Modern springs in Grand Canyon reflect mixing of deeply derived (endogenic) fluids with meteoric (epigenic) recharge. Travertine (<1 Ma) and speleothems (2–4 Ma) yield $^{87}Sr/^{86}Sr$ and $\delta^{13}C$ and $\delta^{18}O$ values that overlap with associated water values, providing justification for use of carbonates as a proxy for the waters from which they were deposited. The Hualapai Limestone (12–6 Ma) and Bouse Formation (5.6–4.8 Ma) record paleohydrology immediately prior to and during integration of the Colorado River. The Hualapai Limestone was deposited from 12 Ma (new ash age) to 6 Ma; carbonates thicken eastward to ~210 m toward the Grand Wash fault, suggesting that deposition was synchronous with fault slip. A fanning-dip geometry is suggested by correlation of ashes between subbasins using tephrochronology. New detrital-zircon ages are consistent with the "Muddy Creek constraint," which posits that Grand Wash Trough was internally drained prior to 6 Ma, with limited or no Colorado Plateau detritus, and that Grand Wash basin was sedimentologically distinct from Gregg and Temple basins until after 6 Ma. New isotopic data from Hualapai Limestone of Grand Wash basin show values and ranges of $^{87}Sr/^{86}Sr$, $\delta^{13}C$, and $\delta^{18}O$ that are similar to Grand Canyon springs and travertines, suggesting a long-lived spring-fed lake/marsh system sourced from western Colorado Plateau groundwater. Progressive up-section decrease in $^{87}Sr/^{86}Sr$ and $\delta^{13}C$ and increase in $\delta^{18}O$ in the uppermost 50 m of the Hualapai Limestone indicate an increase in meteoric water relative to endogenic inputs, which we interpret to record progressively increased input of high-elevation Colorado Plateau groundwater from ca. 8 to 6 Ma. Grand Wash, Hualapai, Gregg, and Temple basins, although potentially connected by groundwater, were hydrochemically distinct basins before ca. 6 Ma. The $^{87}Sr/^{86}Sr$, $\delta^{13}C$, and $\delta^{18}O$ chemostratigraphic trends are compatible with a model for downward integration of Hualapai basins by groundwater sapping and lake spillover.

The Bouse Limestone (5.6–4.8 Ma) was also deposited in several hydrochemically distinct basins separated by bedrock divides. Northern Bouse basins (Cottonwood, Mojave, Havasu) have carbonate chemistry that is nonmarine. The $^{87}Sr/^{86}Sr$ data suggest that water in these basins was derived from mixing of high-$^{87}Sr/^{86}Sr$ Lake Hualapai waters with lower-$^{87}Sr/^{86}Sr$, first-arriving "Colorado River" waters. Covariation trends of $\delta^{13}C$ and $\delta^{18}O$ suggest that newly integrated Grand Wash, Gregg, and Temple basin waters were integrated downward to the Cottonwood and Mojave basins at ca. 5–6 Ma. Southern, potentially younger Bouse basins are distinct hydrochemically from each other, which suggests incomplete mixing during continued downward integration of internally drained basins. Bouse carbonates display a southward trend toward less radiogenic $^{87}Sr/^{86}Sr$ values, higher [Sr], and heavier $\delta^{18}O$ that we attribute to an increased proportion of Colorado River water through time plus increased evaporation from north to south. The $\delta^{13}C$ and $\delta^{18}O$ trends suggest alternating closed and open systems in progressively lower (southern) basins. We interpret existing data to permit the interpretation that the southernmost Blythe basin may have had intermittent mixing with marine water based on $\delta^{13}C$ and $\delta^{18}O$ covariation trends, sedimentology, and paleontology. [Sr] versus $^{87}Sr/^{86}Sr$ modeling suggests that southern Blythe basin $^{87}Sr/^{86}Sr$ values of ~0.710–0.711 could be produced by 25%–75% seawater mixed with river water (depending on [Sr] assumptions) in a delta–marine estuary system.

We suggest several refinements to the "lake fill-and-spill" downward integration model for the Colorado River: (1) Lake Hualapai was fed by western Colorado Plateau groundwater from 12 to 8 Ma; (2) high-elevation Colorado Plateau groundwater was progressively introduced to Lake Hualapai from ca. 8 to 6 Ma; (3) Colorado River water arrived at ca. 5–6 Ma; and (4) the combined inputs led to downward integration by a combination of groundwater sapping and sequential lake spillover that first delivered Colorado Plateau water and detritus to the Salton Trough at ca. 5.3 Ma. We propose that the groundwater sapping mechanism strongly influenced lake evolution of the Hualapai and Bouse Limestones and that

Geosphere; June 2015; v. 11; no. 3; p. 660–682; doi:10.1130/GES01073.1; 17 figures; 5 supplemental tables.
Received 16 May 2014 ♦ Revision received 17 January 2015 ♦ Accepted 19 March 2015 ♦ Published online 13 May 2015

groundwater flow from the Colorado Plateau to Grand Wash Trough led to Colorado River integration.

INTRODUCTION

Late Miocene to modern carbonate deposits along the lower Colorado River (Fig. 1) provide a rich source of information about the paleohydrology of spring, lake, and river waters in this region over the past 12 Ma. Recent models for the Bouse Formation have inferred a series of events that took place during a short period of time (bracketed between 5.6 and 4.8 Ma), when first-arriving Colorado River water caused a chain of lakes and internally drained basins to progressively fill and spill in a downward-propagating sequence (Blackwelder, 1934; Spencer and Patchett, 1997; House et al., 2005, 2008; House and Pearthree, 2014; Roskowski et al., 2010; Spencer et al., 2008, 2013). The Bouse Formation provides a record of these events, which some studies conclude took place in less than 50–100 ka (Spencer et al., 2008). The inferred "event stratigraphy" of the Bouse Formation challenges notions of Walther's law, the resolution of available geochronology, and time scales needed for establishment of continental-scale river systems. Earlier models for deposition of all of the Bouse and Hualapai Limestones in a marine estuary (e.g., Metzger, 1968; Smith, 1970; Buising, 1988, 1990) have been more recently refuted based on isotopic and stratigraphic data (Spencer and Patchett, 1997; Roskowski et al., 2010; Spencer et al., 2013; Pearthree and House, 2014). However, a marine influence in the southernmost Bouse basins is still supported by some data sets (McDougall, 2008, 2010; McDougall and Miranda Martinez, 2014). Resolution of the debate about a possible marine connection for the southern Blythe basin is needed in order to test competing models for the magnitude of post–6 Ma uplift of the Colorado Plateau relative to the sea level (e.g., Lucchitta, 1979; Karlstrom et al., 2007, 2008).

This paper uses new and previously published data on the geochemistry of carbonates to test and refine models for initiation of the Colorado River by downward integration, and explore the possibility of a marine influence in southernmost exposures of the Bouse Formation. We applied multiple geochemical tracers—$^{87}Sr/^{86}Sr$; [Sr], $\delta^{13}C$, and $\delta^{18}O$—to characterize the geochemistry of waters and carbonates in the southwestern Colorado Plateau region over the past 12 Ma We first characterized modern springs and surface waters of the Grand Canyon region to develop a snapshot of the modern hydrologic system. We then extended this snapshot back in time to about ca. 1 Ma, by showing that Qua-

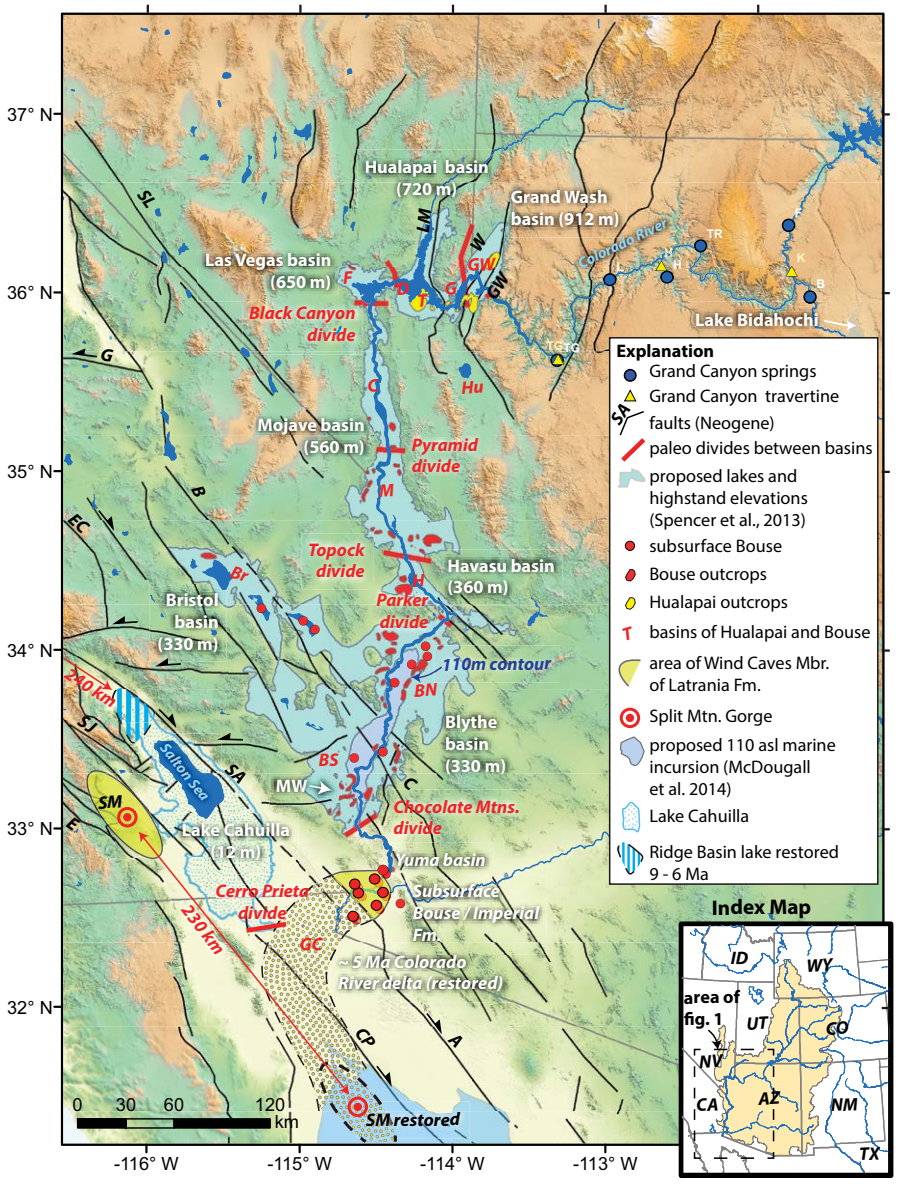

Figure 1. Map of the Grand Canyon and lower Colorado River region with inferred Bidahochi, Hualapai, and Bouse paleolakes. Labeled springs (blue dots in Grand Canyon) are: B—Blue Spring, F—Fence, TR—Thunder River, H—Havasu, L—Lava Warm Spring, TG—Travertine Grotto. Labeled travertines (yellow triangles in Grand Canyon) are: K—Kwagunt, H—Havasu, TG—Travertine Grotto. Surface exposures of the Hualapai Limestone are yellow; Bouse Formation are red; red dots show drill holes that encountered Bouse Formation. Paleolake maximum elevations are from Spencer et al. (2008, 2013) and Pearthree and House (2014). SM—Split Mountain Gorge outcrops of Imperial Formation (solid line) restored 230 km to the SE (dashed line) (Dorsey et al., 2007; Dorsey, 2012). Miocene Ridge basin restored ~240 km (Talbot, 1994). Labeled faults were active in the past 6 Ma. State abbreviations: ID—Idaho, WY—Wyoming, UT—Utah, NV—Nevada, CA—California, CO—Colorado, AZ—Arizona, NM—New Mexico, TX—Texas. Fault abbreviations: A—Altar, B—Bristol, C—Cibola, CP—Cerro Prieto, E—Elsinore, EC—Eastern California shear zone, G—Garlock, LM—Lakeside Mine, SA—San Andreas, SJ—San Jacinto, SL—State Line, W—Wheeler. Basin abbreviations: Br—Bristol, BN—northern Blythe, BS—southern Blythe, C—Cottonwood, D—Detrital, F—Frenchman, G—Gregg, GC—Gulf of California, GW—Grand Wash, H—Havasu, Hu—Hualapai, M—Mojave, SM—Split Mountain, and T—Temple.

ternary travertines associated with modern carbonic spring systems have an isotopic character similar to associated waters, and thus these carbonates provide a reasonable approximation of ancient spring-water chemistry. We extended this reasoning further back in time and compared the geochemistry of 2–4 Ma U-Pb–dated groundwater speleothems in Grand Canyon. Finally, we present new and previously published data for the geochemistry of carbonates from the late Miocene to early Pliocene Hualapai Limestone and Bouse Formation, including new measured sections and chemostratigraphy for the Hualapai Limestone. Our organization of topics "follows the water" in a general progression from upstream to downstream.

It is widely agreed that the Hualapai Limestone at the western mouth of Grand Canyon was deposited between 12 and 6 Ma, prior to the arrival of the Colorado River at ca. 5–6 Ma (Spencer et al., 2013). There is ongoing debate, however, regarding the exact age and early history of the Colorado River (Dorsey et al., 2007, 2011; House et al., 2008; Aslan et al., 2010; Spencer et al., 2013; Miller et al., 2014; Pearthree and House, 2014; McDougall and Miranda Martinez, 2014; Harvey, 2014). In this paper, we adopt the view that the first Colorado River waters reached the western edge of the Colorado Plateau after 6 Ma (e.g., the age of upper Hualapai Limestone; Spencer et al., 2001) and before the ca. 4.4 Ma river gravels at the western mouth of Grand Canyon (Faulds et al., 2001). The goals of this paper are to present a new model for the importance of groundwater during Colorado River integration, reinforce published models for downward integration of the river through a series of lakes, and depart from some recent models by showing that existing data permit an intermittent marine influence on the southernmost basin of the Bouse Formation.

METHODS

Twenty-three new Sr isotope analyses were conducted on a Neptune multicollector–inductively coupled plasma–mass spectrometer (MC-ICP-MS) at the Radiogenic Isotope Geochemistry Laboratory in the Department of Earth and Planetary Sciences at the University of New Mexico. Samples of 30–40 g of calcite were dissolved in 3 *N* HNO_3, run through a 200 µl Teflon column with Eichrom Sr-spec resin, dried, and then redissolved in 3% HNO_3 acid. They were introduced into a Cetac Aridus II desolvating nebulizer and run against National Bureau of Standards Sr standard NBS-987, which has an $^{87}Sr/^{86}Sr$ value of 0.71025. Values are reported with 1σ (%) standard error. These data were combined with a comprehensive compilation of ~200 $^{87}Sr/^{86}Sr$ analyses on waters and ~250 on carbonates from the region (summarized in Supplemental Table 1[1]). Our simple two-component Sr isotope mixing models using the $^{87}Sr/^{86}Sr$ ratio and [Sr] concentrations follow the methods of Ingram and DePaolo (1993) and Crossey et al. (2006).

In total, 230 samples were run for stable oxygen and carbon isotopic analysis; these were drilled, and powders were flushed with He gas and then reacted for 24 h with H_3PO_4 at 50 °C (Spotl and Vennemann, 2003). Evolved CO_2 was measured by continuous-flow–isotope ratio–mass spectrometry using a Gasbench device coupled to a Finnigan Mat Delta Plus Isotope Ratio Mass Spectrometer at the Stable Isotope Laboratory at the University of New Mexico. Oxygen isotope ratios in waters were determined using the CO_2 equilibration technique and are reported using the standard delta notation versus Vienna standard mean ocean water (V-SMOW) with a precision of ±0.3‰. Hydrogen isotope ratios were measured using the continuous-flow high-temperature reduction method using a temperature conversion elemental analyzer (TC/EA) coupled to a Delta Plus XL Thermo-Finnigan mass spectrometer. Carbon results are reported in ‰ relative to Peedee belemnite (PDB) with a precision of ±0.3‰. These data were combined with a comprehensive compilation of water and carbonate stable isotope data from the region (summarized in Supplemental Table 1 [see footnote 1]).

Six tephra samples were sent to the U.S. Geological Survey (USGS) laboratory for chemical correlation. Three yielded sufficient glass shards to provide correlation information. Nine major elements (SiO_2, Al_2O_3, FeO, MgO, MnO, CaO, TiO_2, N_2O, and K_2O) were analyzed using the electron microprobe. The raw data were then recalculated to 100% on a fluid-free basis. Coefficient analysis was performed on the chemical data, and the normalized values were compared to a database (~5800) of chemical "fingerprints" in the USGS Tephrochronology Project reference database. For complete tephrochronology interpretation, independent age control, stratigraphic position, field, petrologic characteristics, and mineralogy were also considered. Supplemental Table 2[2] summarizes raw and normalized chemical data, comparative chemical data, and lists of chemical correlatives.

U/Pb dating of carbonates may offer a new tool for refining the age and duration of deposition of the Hualapai Limestone and Bouse Formation. Samples were cut out with a rock saw, etched in weak (~1 *N*) HNO_3 for <30 s, washed with 18 MΩ H_2O, dried, and then broken into small pieces with an agate mortar and pestle. Five representative pieces (each with a mass of 30–70 mg) were dissolved separately in 15 *N* HNO_3, spiked with ^{205}Pb, fluxed for >1 h, dried, dissolved in 6 *N* HCl, dried again, dissolved in 2 *N* HCl, dried once more, and then dissolved in 1 *N* HBr. Each sample was then cleaned, and U, Th, and Pb were separated using anion resins. U, Th, and Pb ratios were measured with Neptune MC-ICP-MS. All appropriate ratios were corrected for excess ^{206}Pb from initial ^{234}U by assuming an initial $\delta^{234}U$ value of 750‰. Raw data were reduced using PBDATA (Ludwig, 1993) and a Pb blank of ~10 pg. U-Pb ages were generated using ISOPLOT (Ludwig, 2001). Ages are reported as U-Pb concordia-linear dates, and data reported in Supplemental Table 3[3].

U-Pb analyses of individual detrital zircons were obtained by laser ablation–inductively coupled plasma–mass spectrometry (ICP-MS) at the University of Arizona LaserChron Center. Laser ablation was conducted with an Excimer laser beam diameter of 30 or 35 µm and a pulse frequency of 7 Hz. Measurements were performed with the Nu high-resolution (HR) MC-ICP-MS system (Gehrels et al., 2008; Gehrels and Pecha, 2014). Analysis sites were randomly targeted. Most zircon yielded U-Pb results that were concordant to within 10%. Complete data tables, evaluation of the 49,127 secondary standard data points, and the basis for making statistical comparisons between samples are provided in Supplemental Table 4[4]. All location data for new geochronology samples and measured sections are in Supplemental Table 5[5].

[1]Supplemental Table 1. Water and carbonate chemistry from the Grand Canyon–Colorado River region. If you are viewing the PDF of this paper or reading it offline, please visit http://dx.doi.org/10.1130/GES01073.S1 or the full-text article on www.gsapubs.org to view Supplemental Table 1.

[2]Supplemental Table 2. U.S. Geological Survey tephrochronology report. If you are viewing the PDF of this paper or reading it offline, please visit http://dx.doi.org/10.1130/GES01073.S2 or the full-text article on www.gsapubs.org to view Supplemental Table 2.

[3]Supplemental Table 3. Data from U-Pb dating of carbonate. If you are viewing the PDF of this paper or reading it offline, please visit http://dx.doi.org/10.1130/GES01073.S3 or the full-text article on www.gsapubs.org to view Supplemental Table 3.

[4]Supplemental Table 4. U-Pb geochronologic data from detrital zircons and Gold Butte Granite. If you are viewing the PDF of this paper or reading it offline, please visit http://dx.doi.org/10.1130/GES01073.S4 or the full-text article on www.gsapubs.org to view Supplemental Table 4.

[5]Supplemental Table 5. Location data for geochronology samples and measured sections. If you are viewing the PDF of this paper or reading it offline, please visit http://dx.doi.org/10.1130/GES01073.S5 or the full-text article on www.gsapubs.org to view Supplemental Table 5.

GEOCHEMISTRY: BACKGROUND AND DATA COMPILATIONS

Strontium Concentration and Isotopic Ratios

Calcite contains a wealth of semi-independent tracers. The $^{87}Sr/^{86}Sr$ ratios combined with Sr concentration, [Sr], in waters can faithfully record the nature of source waters and mixtures of different water sources because [Sr] abundance is variable, $^{87}Sr/^{86}Sr$ ratios are precisely measured, and because different source regions have characteristically different ranges of values. The $^{87}Sr/^{86}Sr$ ratios in carbonates tend to be a direct reflection of paleowater chemistry because Ca and Sr readily substitute in carbonate rocks. This is demonstrated by data that show similar $^{87}Sr/^{86}Sr$ values in modern waters and their associated travertine deposits (Crossey et al., 2006).

The $^{87}Sr/^{86}Sr$ ratio provides a key data set with which to evaluate modern waters and modern to ancient carbonate deposits (Spencer et al., 2013, and references therein), because $^{87}Sr/^{86}Sr$ is a conservative tracer, and values measured in carbonates mimic the $^{87}Sr/^{86}Sr$ composition of the water from which they were deposited (Ingram and DePaolo, 1993; Spencer and Patchett, 1997; Spencer et al., 2001; Li et al., 2008a; Crossey et al., 2006). However, we also note two significant caveats and potential problems with using $^{87}Sr/^{86}Sr$ as a single tracer without other information: (1) Addition of a small volume of high-$^{87}Sr/^{86}Sr$, high-[Sr] water to low-[Sr] water can have strong leverage on Sr isotope composition; and (2) well-mixed waters should have relatively narrow ranges of $^{87}Sr/^{86}Sr$ (0.0002 for Salton Sea; Li et al., 2008b), whereas lake and river systems with distinct subbasins and substantial input from different source waters often show greater variation; for example, Great Salt Lake waters vary by 0.006 (Fig. 2; Hart et al., 2004) and the San Francisco Bay estuary system varies by 0.004 (Ingram and Sloan, 1992; Ingram and DePaolo, 1993).

Figure 2 provides a synthesis of new and previously published data for $^{87}Sr/^{86}Sr$ in modern waters and Pliocene carbonates of the Colorado River system. The $^{87}Sr/^{86}Sr$ ratios from modern waters in endogenic springs sourced in granitic basement of western Grand Canyon are as high as 0.735. These spring waters mix within the regional groundwater system to produce the extremely wide range of $^{87}Sr/^{86}Sr$ measured in modern springs and travertines of Grand Canyon (0.708–0.735; Crossey et al., 2006). Speleothem values are 0.713–0.723 (Hill et al., 2008); these are from mammillary coatings on caves interpreted to form near the water table in phreatic groundwater cave systems. Hualapai Limestone $^{87}Sr/^{86}Sr$ ranges from 0.7114 to 0.7190, and Bouse carbonates are 0.7100–0.07125 (Spencer and Patchett, 1997; Roskowski et al., 2010). Values distinctly higher than marine values of 0.709 provide evidence that most or all of the Bouse and Hualapai Limestones were deposited in lacustrine rather than marine waters (Fig. 2; Spencer and Patchett, 1997). New results are discussed more fully later herein for modern waters and carbonates from the Hualapai Limestone and Bouse Formation.

Oxygen and Carbon Isotopes

The $\delta^{18}O$ and $\delta^{13}C$ values in travertines exhibit the widest variation in isotopic character of any rock type (Sharp, 2007). Prior work on $\delta^{18}O$ and $\delta^{13}C$ in waters and calcite of the Colorado River system includes studies by Faulds et al. (2001), Gross et al. (2001), Poulson and John (2003), and Roskowski et al. (2010).

Figure 3 shows covariation trends of $\delta^{18}O$ and $\delta^{13}C$ from previously published studies of carbonates precipitated from selected lakes and estuaries in the western United States. Marls that precipitate in the water column and settle as pelagic rain have long been used as proxies for the water chemistry; stromatolites, oncolites, and sometimes shells and tufas can also be used to estimate $\delta^{18}O$ of waters, although their $\delta^{13}C$ can be shifted due to fractionation effects (Talbot, 1990). The different covariation trends in closed basins can be used to characterize the hydrologic setting of internally drained basins (Talbot, 1990). The $\delta^{18}O$ of lake waters primarily reflects elevation (latitude) of recharge and degree of evaporation (i.e., whether the lake is open or closed). The $\delta^{13}C$ in southwestern lakes reflects surface water and groundwater mixing, and then local degassing and related fractionation of $\delta^{13}C$, primary biogenic activity, and decreasing surface area/depth of lakes (Fig. 3). As examples pertinent to this study, Great Salt Lake and Lake Bonneville data show a covariation trend ($r^2 = 0.89$) that reflects a similar mix of recharge waters over the past 17 Ma and strong evaporative fractionation (Talbot, 1990). Shells from Holocene Lake Cahuilla, which formed by flooding of dominantly Colorado River water into the Salton Trough intermittently in the past 20 ka, show a covariation trend ($r^2 = 0.79$) that records evaporation in a closed lake (Li et al., 2008a). Shells from the modern San Francisco Bay (and dating to 2 ka) show weaker covariation ($r^2 = 0.5$) interpreted to reflect changes in salinity due to variable mixing of riverine water and seawater in an open (flow-through) marine estuary (Ingram et al., 1996).

A realignment of covariation trends can record changes in basin chemistry through time. For example, a marked up-section change is seen in the late Miocene (9–6 Ma) Ridge basin (Talbot, 1994). This basin is pertinent because it restores to a geographic position adjacent to the Eastern Transverse Ranges (Fig. 1), and its upper part was contemporaneous with the lower Imperial Formation (e.g., Dorsey et al., 2007). The lower part of the section has nearly constant $\delta^{18}O$, reflecting source waters with variation in $\delta^{13}C$ interpreted to record rapid flow-through in an open lake. The upper covariation segment ($r^2 = 0.84$) is interpreted to record evaporation in a closed lake (Fig. 3; Talbot, 1994). Another example of processes that change the position of collinear arrays is suggested by the difference in published stable isotope values between carbonates of the Hualapai Limestone and Bouse Formation (Roskowski et al., 2010), which reveal an overall shift to the lower right (Fig. 3). This shift may provide information about residence and surface area/depth ratios (e.g., Talbot, 1994) in successively lower lake basins of a developing Colorado River–fed chain of lakes, as discussed in more detail later herein.

Hydrochemistry of Modern Spring Waters

The geochemistry of modern waters in the Grand Canyon region is summarized in Figures 2 and 4, and data are listed in Supplemental Table 1 (see footnote 1; new data are in bold). Figure 2 shows $^{87}Sr/^{86}Sr$ values of the Colorado River, its tributaries, and springs, including labeled springs and spring groups that characterize the largest volume of groundwater inputs such as Fence Springs and Blue Springs of eastern Grand Canyon, Havasu Spring of central Grand Canyon, and Lava Warm Spring and Travertine Grotto Spring of western Grand Canyon. The highly variable $^{87}Sr/^{86}Sr$ values in waters are interpreted to reflect complex mixing of deeply sourced (endogenic) waters, karst aquifer groundwater, and meteoric (epigenic) waters (Crossey et al., 2006). Ranges of $^{87}Sr/^{86}Sr$ values get wider and values are more radiogenic in the western Grand Canyon (Crossey et al., 2009). [Sr] in Colorado River surface water increases from <1 ppm in the eastern Grand Canyon to 1.2 ppm in Lake Mead. Spring waters range from <1 ppm to as much as 15 ppm (Supplemental Table 1 [see footnote 1]). Compiled surface-water (tributary) inputs like the San Juan, Little Colorado, and Virgin Rivers are variable but significantly less radiogenic than groundwater inputs.

Figure 4 shows previously published and new $\delta^{18}O$ and $\delta^{13}C$ stable isotope data from Grand Canyon area waters (blue symbols). Measured water values (relative to SMOW) were converted to values for the carbonate (in PDB) that

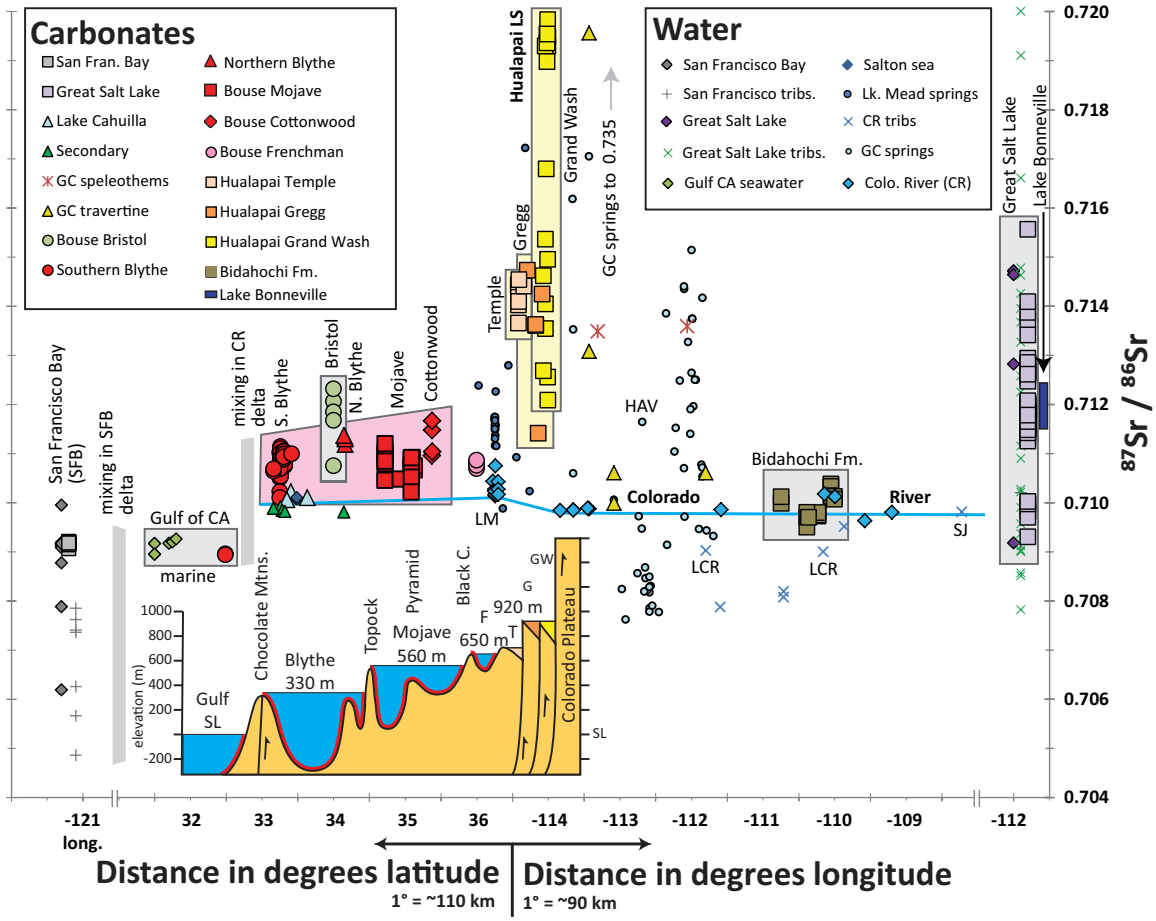

Figure 2. $^{87}Sr/^{86}Sr$ in waters and carbonates from the Colorado River region plotted relative to latitude east of Hoover Dam (Black Canyon divide) and relative to longitude south of Hoover Dam. Modern Colorado River $^{87}Sr/^{86}Sr$ values are shown in solid line, but note variability of Lake Mead (LM) waters. Grand Canyon (GC) springs (small circles) are highly variable and get as radiogenic as 0.735 in western Grand Canyon; HAV—Havasu Spring. Labeled tributaries to Colorado River (CR) are: LCR—Little Colorado River; SJ—San Juan River. Travertines and speleothems overlap with spring values and become more radiogenic in western Grand Canyon. Carbonates of Lakes Bidahochi (ca. 13–11 Ma), Hualapai (12–6 Ma), and Bouse (5.8–4.8 Ma) have distinctive $^{87}Sr/^{86}Sr$ signatures and differ from Gulf of California (CA) marine waters as well as from the 5–6 Ma Imperial Formation marine carbonates. Range of values resulting from mixing for the Great Salt Lake–Lake Bonneville system is shown for comparison to Hualapai variability. Mixing of rivers with seawater in the San Francisco Bay (SFB) estuary may be a "reverse" analog to mixing in the Pliocene Colorado River delta, as rivers in the former are less, rather than more, radiogenic than seawater. Inset shows the fill-and-spill model of downward integration of lakes (Spencer et al., 2013) and important divides of the Hualapai Limestone–Bouse Formation systems, keyed to Figure 1. Red line—hypothesized drape of thin Bouse carbonates in lakes (Pearthree and House, 2014); F—Frenchman basin, G—Gregg basin, GW—Grand Wash, HAV—Havasu Spring, LM—Lake Mead, SL—sea level, and T—Temple basin.

would precipitate from the water at 15 °C based on the models from Demeny et al. (2010) for $\delta^{18}O$ and from Romanek et al. (1992) for $\delta^{13}C$. Similar to $^{87}Sr/^{86}Sr$, $\delta^{18}O$ and $\delta^{13}C$ are highly variable in Grand Canyon groundwaters due to mixing. For example, a dominantly epigenic (meteoric) spring (Thunder River [TR]) differs from springs with strong endogenic component (Travertine Grotto [TG]). High-volume carbonic springs tend to get more negative in $\delta^{13}C$ from east to west (Blue [B], Havasu [H], Lava [L], Travertine Grotto [TG]) at similar $\delta^{18}O$ values (Fence Spring does not follow this pattern). Water-chemistry data have been used to model $\delta^{13}C$ variation in terms of different sources of carbon for carbonic springs (Crossey et al., 2009). The main sources are: C_{carb} = carbon derived from dissolution of carbonate such as from the karst aquifer; C_{org} = organic-sourced carbon such as from soil; and C_{endo} = endogenic sources of carbon such as from the mantle and magmatic sources. For the springs plotted in Figure 4, the C_{endo} component increases from east to west as follows: Thunder River = 0%; Fence = 27%; Havasu = 42%; Lava = 65%; and Travertine Grotto = 84%, in general agreement with $^{87}Sr/^{86}Sr$ data indicating increasing endogenic fluid inputs in western Grand Canyon springs. Endogenic inputs into the Colorado Plateau groundwater system are geochemically potent, but small volume, such that spring chemistry is quite variable from region to region (Crossey et al., 2006).

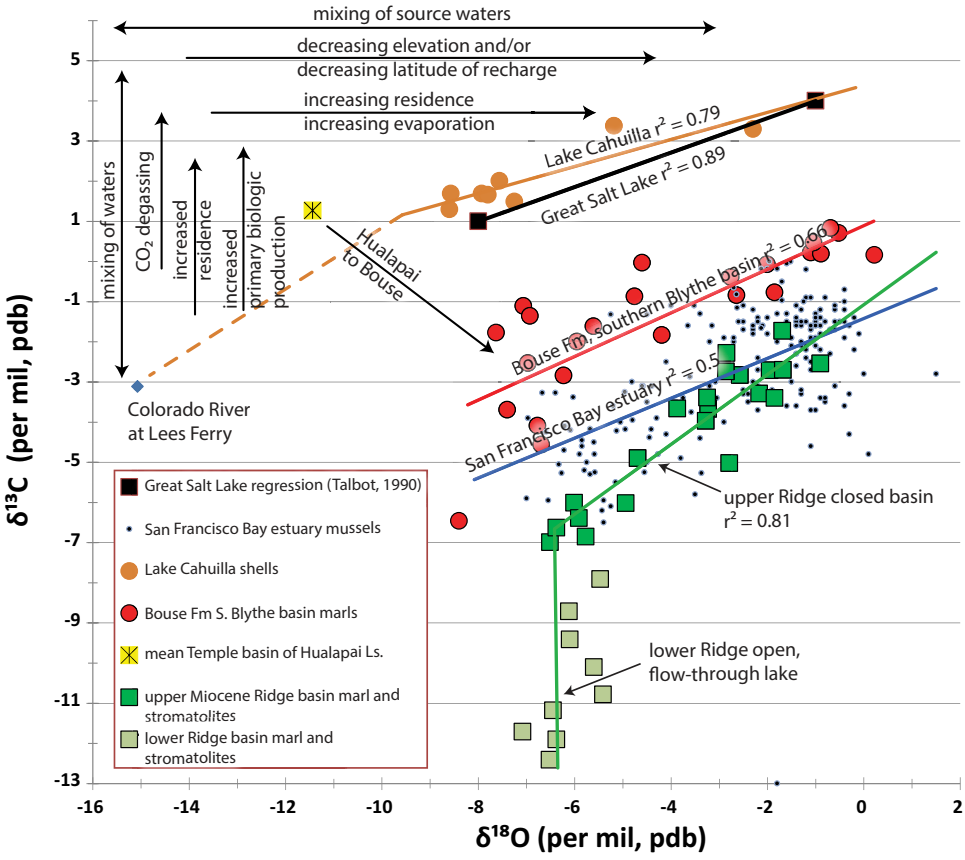

Figure 3. $\delta^{13}C$ and $\delta^{18}O$ covariation in carbonates of the western United States (pdb—Peedee belemnite). Distinct covariation trends may help correlate lake basins, identify different basin hydrochemistry, and evaluate hydrologic separation and basin evolution. Covariation trends with positive slope are commonly interpreted to reflect water evolution in closed basins due to evaporation and other processes shown (from Talbot, 1990). Different basins show distinct trends. Negative slopes can indicate open basin behavior and hydrologic separation (Talbot, 1990). Understanding the negative overall slope from Hualapai to Bouse carbonates motivates later sections of this paper.

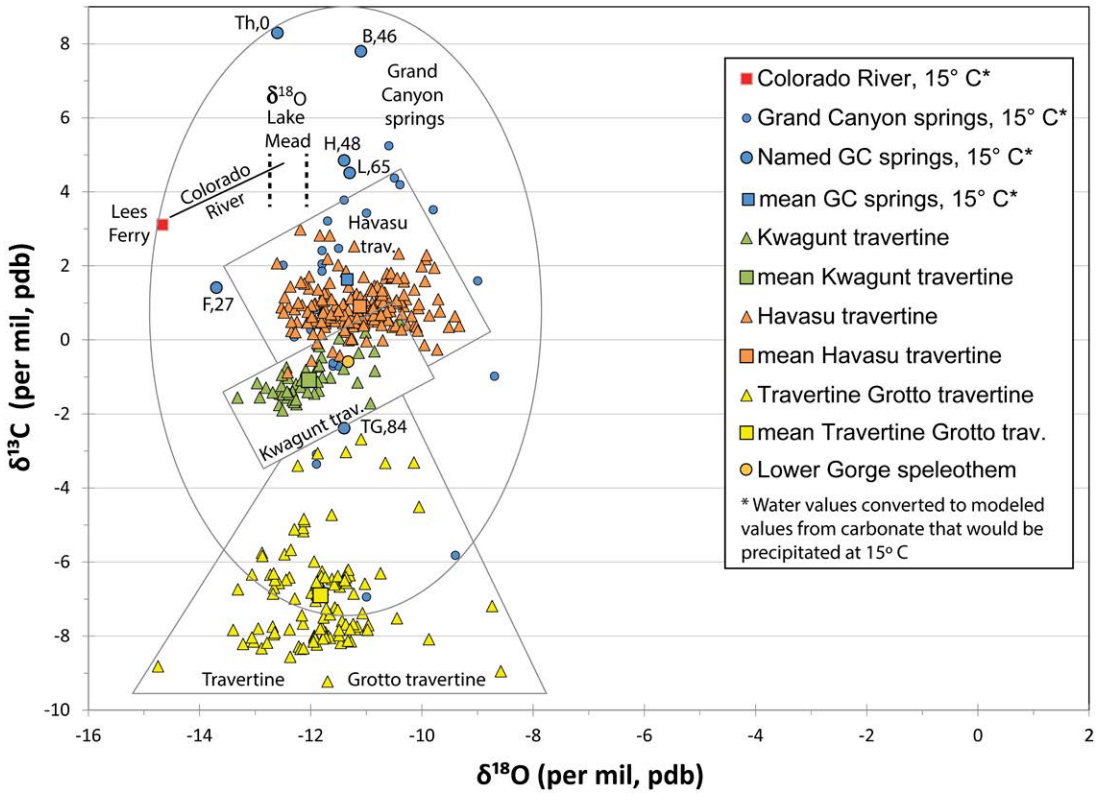

Figure 4. $\delta^{13}C$ vs. $\delta^{18}O$ plot for waters and modern travertines in Grand Canyon (GC) compared to the Colorado River (pdb—Peedee belemnite). Water values were converted to modeled values for the carbonates that would be precipitated from the water using equations from Demeny et al. (2010) for $\delta^{18}O$ and Romanek et al. (1992) for $\delta^{13}C$. Spring and travertine locations keyed to Figure 1 (RM—river miles downstream from Lees Ferry) are: F—Fence Spring (RM 30), K—Kwagunt travertine (green; RM 57), B—Blue Spring (RM 60), TH—Thunder River spring (RM 135), H—Havasu spring and travertine (orange; RM 156), L—Lava Warm Spring (RM 179), TG—Travertine Grotto spring and travertine (yellow; RM 229). Numbers beside labeled springs are the percent of total dissolved inorganic carbon attributed to endogenic sources based on modeled water chemistry (Crossey et al., 2009).

Paleogroundwater $\delta^{18}O$ and $\delta^{13}C$ from Travertine and Speleothems

Figure 4 also plots $\delta^{18}O$-$\delta^{13}C$ values from young (<500 ka) Grand Canyon travertines that are associated spatially with the springs. Travertines show groupings that have heavier $\delta^{13}C$ than their proximal springs, which we interpret to be due to degassing of the light ^{12}C during travertine formation (rather than evaporation, as samples are from high-flow spring vents). The general similarity of arrays between water and travertine for a given region, and the differences between eastern and western Grand Canyon regions, shows that travertine can preserve paleohydrology information back to more than 500 ka.

Kwagunt travertines were deposited ca. 100–400 ka in eastern Grand Canyon (Pederson et al., 2002), and new isotopic data show a covariation array that is interpreted to reflect seasonal variation of groundwaters that were similar to Blue Springs, but with ~8‰–10‰ heavier $\delta^{13}C$ due to degassing during travertine formation. Havasu modern and Quaternary travertines (data from O'Brien, 2002; O'Brien et al., 2006) show ~4‰ heavier $\delta^{13}C$ relative to modern Havasu Spring for the same reason. Travertine Grotto travertines (new data) are also ~5‰ heavier than the carbonates expected to be deposited by Travertine Grotto spring. Nevertheless, the full range of modern spring waters overlaps strongly with the range of Quaternary travertines and a new cave speleothem value from near Rampart Cave of westernmost Grand Canyon (Fig. 4), supporting the use of $\delta^{18}O$-$\delta^{13}C$ values in carbonates as a proxy for the hydrochemistry of the water from which they were deposited, as has also been well established in other studies (Talbot, 1990).

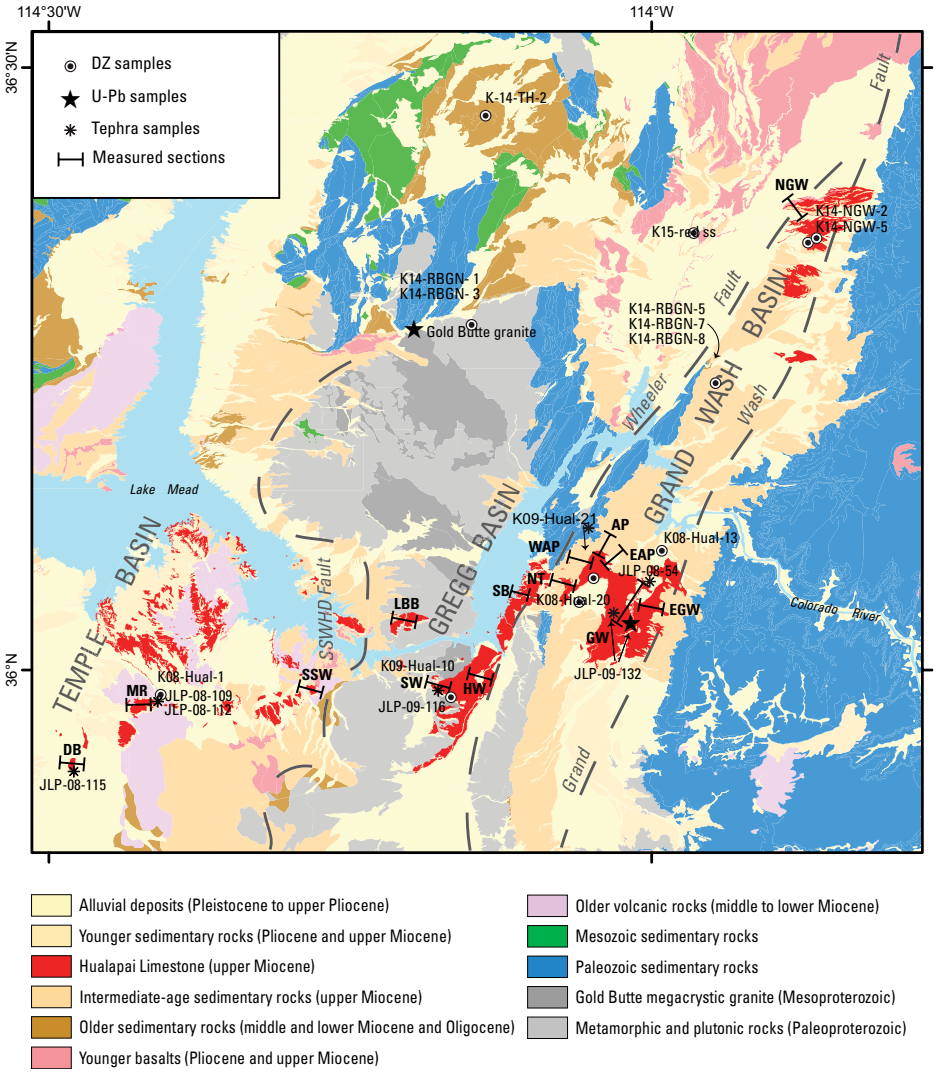

Figure 5. Geologic map of the Lake Mead region (Felger and Beard, 2010) showing locations of measured sections, tephrochronology samples, detrital-zircon (DZ) samples, and U-Pb samples (Hualapai Limestone and Gold Butte granite) that are reported in this paper. Measured sections keyed to Figure 6 are: AP—Airport Point, DB—Detrital basin, EGW—eastern Grand Wash, GW—Grapevine Wash, HW—Hualapai Wash, LBB—Little Burro Bay, MR—Mine Road, NGW—northern Grand Wash, NT—North Tower, SB—Smith Bay, SSW—Salt Spring Wash, SW—Spring Wash, EAP—East Airport Point, and WAP—West Airport Point.

HUALAPAI LIMESTONE (12–6 Ma)

Geochronology

The Hualapai Limestone (Blackwelder, 1934; Lucchitta, 1966, 1972; Blair and Armstrong, 1979) was deposited during the interval 12–6 Ma (Spencer et al., 2001) and is preserved in outcrops that roughly encompass the region of Lake Mead, from immediately west of the mouth of Grand Canyon to the upper end of Black Canyon (Fig. 5). These freshwater carbonates rest on locally derived fanglomerate and red siltstone that have variably been called Muddy Creek Formation (Lucchitta, 2013; see nomenclature discussion in Young, 2008), rocks of Grand Wash Trough (Bohannon, 1984), and rocks of Overton Arm (Beard et al., 2007). In contrast to Young (2008), we use the local names and recommend that propagation of the name Muddy Creek Formation outside of the Virgin River depression should be abandoned because of the sedimentary and tectonic complexity of internally drained basins of the Grand Wash region (see Dickinson et al., 2014). Here, we use the term Hualapai Limestone for the interbedded carbonates and red siliciclastic rocks above the first appearing limestone in each measured section.

Our new measured sections (for locations, see Fig. 5; Supplemental Table 5 [see footnote 5]) show that carbonates are interbedded with red siltstones in all sections (Fig. 6; Faulds et al., 2001; Wallace et al., 2005; Pearce, 2010) in a series of fault-bounded basins (Lucchitta, 1972; Seixas et al., 2015). The thickness of the Hualapai Limestone varies in different basins and reaches a maximum of 210 m in eastern Grand Wash basin near the mouth of Grand Canyon. This location makes it useful for understanding the history of integration of the Colorado River through western Grand Canyon.

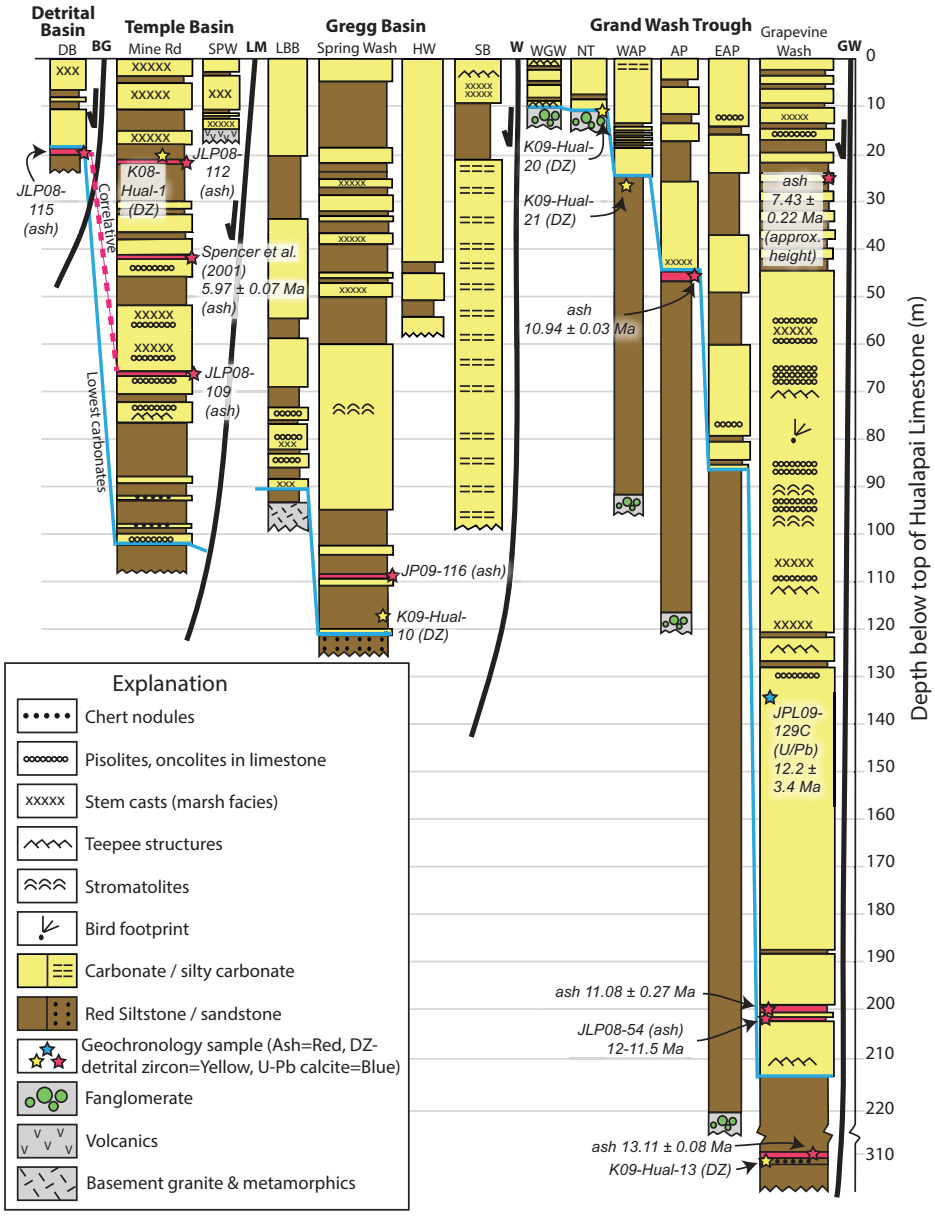

Figure 6. Measured stratigraphic sections of the Hualapai Limestone showing thicker sections in eastern parts of each half graben basin and an overall thickening in eastern basins (modified from Pearce, 2010). All sections are characterized by interlayered shallow-water lacustrine/marsh carbonate and fine-grained red siltstones (sedimentary facies described in Pearce, 2010; Seixas et al., 2015). Tephrochronology samples (yellow stars) are summarized in Supplemental Table 2 (see text footnote 2); note the red dashed line reflects samples that correlate with each other but did not yield regional age correlations. This and other geochronologic controls show tilt-fanning of depositional time lines. Detrital-zircon age spectra (yellow stars) are summarized in Figure 9 and Supplemental Table 3 (see text footnote 3). Sections are hung from the exposed top of each section, which are correlated to each other and interpreted as the time of last carbonate deposition before integration of the Colorado River through all three basins at ca. 6 Ma (Spencer et al., 2001). Section abbreviations are: AP—Airport Point, DB—Detrital basin, HW—Hualapai Wash, LBB—Little Burro Bay, NT—North Tower, SPW—Salt Spring Wash, SB—Smith Bay, EAP—East Airport Point, WAP—West Airport Point, and WGW—West Grand Wash. Fault abbreviations are: BG—Blind Goddess, GW—Grand Wash, LM—Lakeside Mine, and W—Wheeler.

Grand Wash basin contains the thickest section (up to 210 m) of Hualapai Limestone. The age constraints on deposition are shown in measured sections of Figure 6. An age of 13.11 Ma from an ash bed in red siltstones ~100 m below the first Hualapai carbonate provides a maximum age on the Hualapai carbonate deposition. A new ash bed sampled in Grapevine Wash ~8 m above the base of the Hualapai Limestone (Fig. 7) is dated at 12.07–11.31 Ma (see following), which now provides the best estimate for the onset of carbonate deposition in Grand Wash Trough. A 10.94 Ma ash age (Wallace et al., 2005) at the red siltstone to carbonate transition in a thinner section at Airport Point (Fig. 6) indicates a time-transgressive onset of carbonate deposition in different parts of the basin. An ash near the top of the Hualapai Limestone in the Grapevine Wash section was dated as 7.43 ± 0.22 Ma (Faulds et al., 2001). If deposition rates were constant, this suggests the 212 m of section could have been deposited between 12 Ma and 7.43 Ma at an average rate of 45 m/Ma Thus, available data suggest that carbonate deposition lasted from 12 to ca. 7 Ma in Grand Wash basin. Measured sections within and between basins are correlated from the exposed tops of the sections (Fig. 6). Temple basin (Mine Road section, Fig. 6) contains the location of the 5.97 Ma ash (Spencer et al., 2001) used for the age of the upper Hualapai Limestone. We recognize that there is a lack of geochronology to prove synchronous deposition, and, even if tops were contemporaneous at ca. 6 Ma, the potential for differential erosion makes this an approximate correlation. If spillover and downward integration models are applied, sedimentation rates may have been faster in Gregg and Temple basins than in Grand Wash basin.

Measured sections in the Hualapai Limestone (Fig. 6; Pearce, 2010) suggest wedge-shaped basin geometries with thickest accumulations on the immediate downthrown side of normal faults. Thickness and facies variations and soft sediment deformation features suggest that the carbonates were deposited syntectonically during slip on the Grand Wash, Wheeler, and Lakeside Mine normal faults (Pearce, 2010; Seixas et al., 2015). We summarize Hualapai Limestone chemostratigraphy and geochronology from east to west using multiple measured sections in each of three adjoining basins: (1) Grand Wash basin, bounded on the east by Grand Wash fault (GW of Fig. 1); (2) Gregg basin, bounded on the east by Wheeler fault (W of Fig. 1); and (3) Temple basin, bounded on the east by the Lakeside Mine fault (LM of Fig. 1). For present purposes, the Hualapai Limestone outcrops in Detrital basin are considered a western part of Temple basin that extends west to a drainage

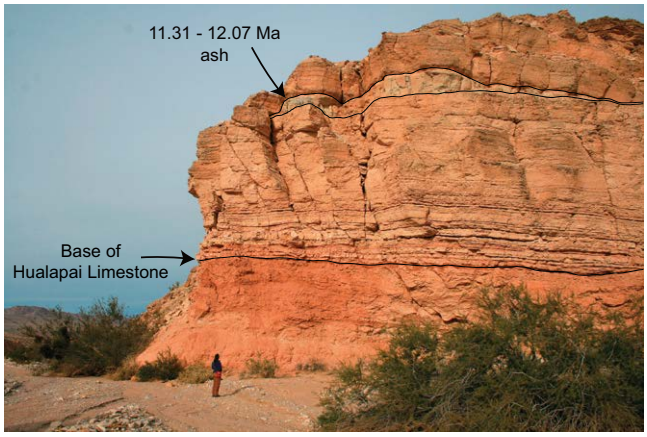

Figure 7. Ash beds and tephrochronology: photograph of the 11.31–12.07 Ma ash bed near the base of the Hualapai Limestone (halfway up the cliff) in Grapevine Gulch. Note person at base of cliff for scale. Base of Hualapai Limestone is also shown.

divide at the upper end of Black Canyon (Fig. 1; Roskowski et al., 2010; Spencer et al., 2013). Sedimentation rates were likely faster in deeper depocenters adjacent to active normal faults, and fanning-dip geometries need to be considered in correlation of measured sections.

Tephrochronology

As summarized in Supplemental Table 2 (see footnote 2), a tephra sample collected from near the base of the Hualapai Limestone in Grand Wash basin (JLP-08–54, Fig. 6) is located several meters above the carbonate–red siltstone contact (Fig. 6). This tephra is chemically similar to tephra derived from the Snake River caldera hotspot of southern Idaho, with closest matches having ages in the range of 12.07–11.31 Ma based on the $^{40}Ar/^{39}Ar$ dated Trapper Creek section (Supplemental Table 2 [see footnote 2]). The sandstone sample is ~2 m below the tephra dated by Wallace et al. (2005) as 11.08 ± 0.27 Ma. The age range of 12.07–11.31 Ma overlaps with this ash but perhaps extends the range of carbonate deposition back to ca. 11.3–12 Ma.

Two additional ashes were sampled. One sample is from near the base of the Hualapai Limestone in the Temple basin, Mine Road section (JLP 08–109), which is ~20 m below a 5.97 Ma ash (Spencer et al., 2001), and one is from the base of the Detrital Wash section (JLP-08–115; Fig. 6). These samples did not yield geochemical correlations with the USGS tephrochronology database, but they had close chemical correlations with each other (similarity coefficient of 0.947; see Supplemental Table 2 [see footnote 2]). This ash thus provides a local time marker that indicates that Detrital basin carbonate deposition began before 6 Ma, when about half (30 m) of the Hualapai Limestone section (carbonates plus red siltstones) had accumulated in the Temple basin. Thus, overall accumulation rates (and thicknesses) in Temple basin were higher than those of Detrital basin. This is compatible with models for increased down-section dips (tilt-fanning) of depositional time lines in each basin and is compatible with integration between basins ca. 6 Ma.

Pilot U-Pb Dating Attempts

Pilot attempts at U/Pb dating of carbonate were performed on several samples from the Hualapai Limestone. The best result came from sample JLP09-129C, which was sampled in Grapevine Wash and consists of a crystalline calcite infilling in micrite (the infilling was analyzed). As shown in Figure 8, this sample yields a three-dimensional isochron age that is consistent, within error, compared to available geochronology. It gives an age of 12.3 ± 3.4 Ma and is stratigraphically between ashes dated at 11 and 7 Ma (Faulds et al., 2001). This age is apparently too old, and its precision too low, to refine this particular section of the Hualapai Limestone. All aliquots yielded positive measured $\delta^{234}U$ values of 13‰–27‰, also permissive of an (improbable) age of younger than ca. 2.5 Ma. Our current interpretation is that the positive $\delta^{234}U$ values indicate secondary precipitation of young (<2.5 Ma) calcite, which will affect the U/Pb ages in, as yet, unconstrained ways. Until the U and Pb concentrations, isotopic composition, and any secondary calcite are better constrained and additional samples are dated in stratigraphic context, this age should be taken as a promising pilot sample, but not an accurate age.

Detrital-Zircon Data

The histories of present and past drainage systems can be interpreted using U-Pb dating of detrital zircons. Recent advances have emerged from increasingly well-understood detrital-zircon signatures for the region. Pertinent data from various units are shown in Figure 9. Cambrian strata of the Colorado Plateau show the restricted Yavapai-Mazatzal (1.7–1.8 Ga) plus 1.46 Ga "twin age peaks" that reflect erosion from Precambrian basement of the transcontinental arch, whereas Upper Paleozoic strata in the walls of Grand Canyon show a strong peak at 1.1 Ga and numerous Paleozoic grains (numbers 1 and 2 of Fig. 9; Gehrels et al., 2011). The Paleocene–Eocene Music Mountain Formation was derived from Precambrian rocks from the Mogollon highlands to the south of the Colorado Plateau and has peaks of 1.70 and 1.41 Ga (Dickinson et al., 2012).

A test of the age, provenance, and degree of connectedness of Grand Wash Trough basinal sediments was conducted for this study using new detrital-zircon data. These data also help test models for an "old" Grand Canyon of 70–50 Ma (Wernicke, 2011; Flowers and Farley, 2012,

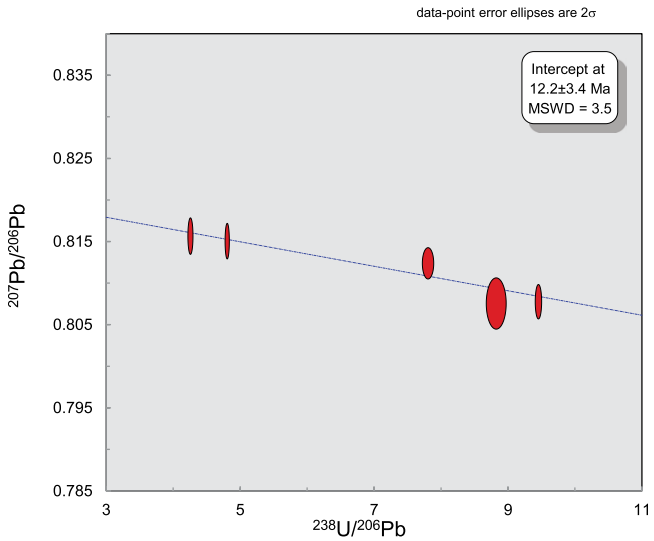

Figure 8. U-Pb concordia-constrained linear three-dimensional isochron (Ludwig, 2001) ages on one sample from the Hualapai Limestone of Grand Wash basin that is within error of tephra constraints and demonstrates potential for refined U-Pb dating of the Hualapai Limestone. MSWD—mean square of weighted deviates.

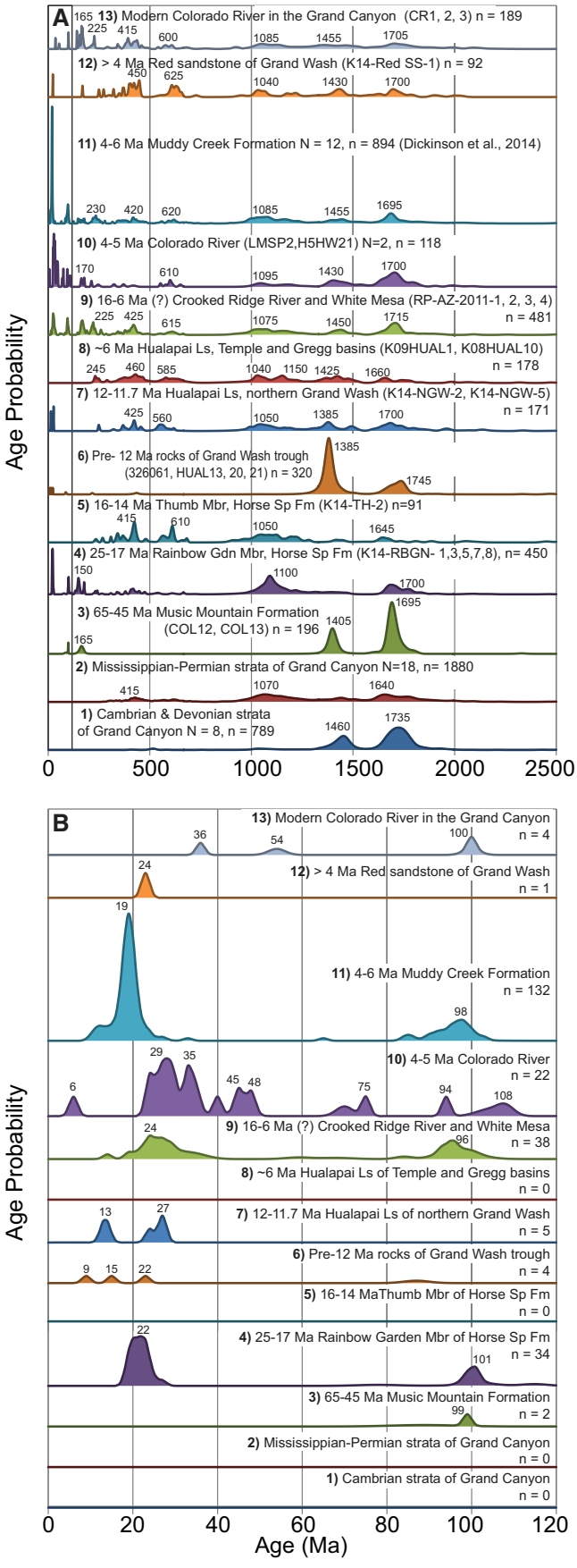

Figure 9. Distributions of U-Pb ages (normative probability plots subtending equal areas beneath curves) for detrital-zircon (DZ) populations in relevant samples from the region. (A) = 2500–0 Ma full grain detrital-zircon spectra. (B) 120–0 Ma young-grain detrital-zircon spectra. 1—potential late Paleozoic source rocks of Grand Canyon (Gehrels et al., 2011); 2—Mississippian to Permian strata from Grand Canyon (Gehrels et al., 2011); 3—65–45 Ma Paleocene–early Eocene Music Mountain Formation (Dickinson et al., 2012); 4—25–17 Ma Rainbow Garden Member of Horse Spring Formation (Lamb et al., 2015; this study); 5—16–14 Ma Thumb Member of Horse Spring Formation (this study); 6—pre–12–7 Ma rocks of Grand Wash Trough (this study), 7—Hualapai Limestone of northern Grand Wash Trough (this study); 8—ca. 6 Ma syn–Hualapai Limestone sandstones of Gregg and Temple basins (this study); 9—16–6 Ma (?) Crooked Ridge River and White Mesa alluvium (Hereford et al., 2015); 10—4–5 Ma Pliocene Colorado River (Kimbrough et al., 2015); 11—4–6 Ma Muddy Creek Formation (Dickinson et al., 2014); 12—Red sandstone from northern Grand Wash Trough; 13—modern Colorado River sands in Grand Canyon (Kimbrough et al., 2015). (C) U-Pb inductively coupled plasma–mass spectrometry age for Gold Butte granite (this study). MSWD—mean square of weighted deviates.

2013) or 17 Ma (Polyak et al. 2008) versus a dominantly "young" western Grand Canyon (Lucchitta, 1966; Karlstrom et al., 2013, 2014). This test relies on the notion that the detrital-zircon makeup of the rocks of Grand Wash Trough that were deposited in the path of the Colorado River from 25 to 6 Ma would be predicted to have appreciable Colorado Plateau–western Grand Canyon–derived detritus in any viable "old" canyon model. New detrital-zircon data are presented in Supplemental Table 4 (see footnote 4).

The 25–17 Ma Rainbow Garden Member of the Horse Spring Formation of the Grand Wash Trough has peaks at 1.70 and 1.1 Ga as well as a syndepositional peak at 20–23 Ma (number 4, Fig. 9). It is interpreted to have been derived from nearby exposures of Lower Mesozoic and Upper Paleozoic strata in adjacent fault blocks with the notable addition of volcanic detritus from the Caliente volcanic field (ca. 19–28 Ma) to the north, but not to have input from the paleo–Colorado River from the east (Lamb et al., 2015). A sample from the 16–14 Ma Thumb Member of the Horse Spring Formation of the Grand Wash Trough (number 5, Fig. 9) has peaks at 1.65, 1.42, 1.05 Ga, and 610 and 415 Ma peaks. An absence of young grains is compatible with models for local derivation in alluvial fans derived from adjacent fault blocks (Beard, 1996).

Four detrital-zircon samples were collected from the rocks of Grand Wash Trough (Bohannon, 1984) that directly underlie the Hualapai Limestone in Grand Wash Trough (number 6, Fig. 9; Kimbrough et al., 2015). The lowest sample (K09-Hual-13) was collected from a sandstone bed that immediately underlies the 13.11 ± 0.08 Ma ash near Pierce Ferry (Fig. 5). This sample is ~100 m below the basal Hualapai Limestone and is directly in the path of the modern Colorado River. Its detrital-zircon spectrum (90 grains) has a bimodal pattern with peaks of 1.38 Ga and 1.72–1.74 Ga (Supplemental Table 3 [see footnote 3]). Three other samples were collected from the western part of Grand Wash basin, just east of the Wheeler fault and immediately below the basal Hualapai Limestone in the thinner stratigraphic sections west of Airport Point (Fig. 6). K09-Hual 20 was collected in coarse fanglomerate that underlies an ~10-m-thick Hualapai Limestone section near the divide between Grand Wash and Gregg basins. K09-Hual 21 was collected near the junction of the South Cove and Pearce Ferry roads in red siltstone that underlies a thin Hualapai Limestone section. An additional sample (32606-1) was collected in approximately the same location as K09-Hual 21 (Kimbrough et al., 2015; Supplemental Table 3 [see footnote 3]). The latter three samples are within the upper 20–30 m of the estimated 6–7 Ma top of the Hualapai Limestone in Grand Wash basin.

K09-13 has a well-constrained age (13 Ma), and all of these lower Grand Wash Trough samples (320 grains; number 6 of Fig. 9) represent deposition of red siltstones and fanglomerates in the Grand Wash Trough from 13 to ca. 7 Ma. Collectively, they show a 1.39 Ga peak that is significantly younger than the 1.45–1.4 Ga peak seen in many successions. Pearce (2010) and Pearce et al. (2011) attributed this to derivation from the 1370–1380 Ma Peacock Mountains Granite (Albin et al., 1991) and other ca. 1.37–1.38 Ga granites to the south (black x's in Fig. 1), but not from western Grand Canyon, as no Paleozoic grains are present. However, a new U-Pb age for the Gold Butte granite near Gold Butte (black star in Fig. 1) gives an age of 1372 ± 12 Ma (Fig. 9C) such that derivation from the local basement to the west seems more likely. The four Grand Wash Trough samples are statistically incongruent (except 326061 and HUAL13, which are virtually identical at $P = 0.99$, and Hual-13 and Hual-21, which are closely similar at $P = 0.37$), but collectively, we use them to provide a net composition for the 12–7 Ma pre–Hualapai Limestone rocks of Grand Wash Trough. These spectra are consistent with the Muddy Creek constraint (Lucchitta, 2013) that, between 13 and 7 Ma, limited, or no, far-traveled detritus from the Colorado Plateau or Grand Canyon reached Grand Wash sediments that were deposited in the direct path of the modern Colorado River where it emerges from Grand Canyon. This conclusion is strengthened by the paucity of 1.0–1.2 Ga, Paleozoic, and Mesozoic grains that are common in both the Paleocene and modern Colorado River. Further, these sediments are unlikely to have been derived from the Music Mountain Formation because of the differences in the "twin age peaks."

We analyzed two samples from a previously unstudied ~40-m-thick carbonate–red siltstone section in the northern Grand Wash Trough (number 7 of Fig. 9) that has interbedded ash layers of 12–11.7 Ma (Billingsley et al., 2004) and correlates with Hualapai Limestone (Felger and Beard, 2010; Figs. 1 and 5). These samples show detrital-zircon peaks somewhat similar to those of southern Grand Wash Trough, including its young grains, but the northern samples differ in having numerous grains of 1.2–1.0 Ga and Paleozoic age. This spectrum is similar to the Rainbow Garden and Thumb Members (numbers 4 and 5 of Fig. 9) and could reflect derivation from the same sources and perhaps local recycling of these nearby 25–14 Ma units.

Figure 9 (number 8) shows a spectrum from two samples of Hualapai Limestone from the Temple and Gregg basins. The Gregg basin sample is from near the base of the Hualapai Limestone, whereas the Temple basin sample is in the middle of the section and ~10 m below the 5.97 Ma tephra (Fig. 6). These spectra are similar enough ($P = 0.7$) to consider them to have been derived from the same population (70% probability). This Temple-Gregg curve generally resembles those in the Rainbow Garden and Thumb Members and the northern Grand Wash Trough, as well as Pliocene–Holocene Colorado River sands (Fig. 9; Kimbrough et al., 2011, 2015), except that the Hualapai Limestone in Gregg and Temple basins lacks age peaks younger than 235 Ma (middle Triassic). Additional analyses are needed to preclude this being a sampling bias, but data so far suggest that no strata younger than Moenkopi Formation were present in the provenance. This is unlike the early Colorado River signature (number 10 of Fig. 9) and suggests that ca. 6 Ma sand in Gregg-Temple basins was derived from Paleozoic and basal Mesozoic strata (Moenkopi Formation contains abundant 245 Ma grains) that overlie Precambrian basement along the flank of the Wheeler Ridge tilt-block between the two basins, thus implying a local provenance west of the Grand Wash Cliffs.

We interpret these data to suggest that, before integration of the different Hualapai Limestone subbasins, sediment was delivered to Grand Wash Trough from the south and west. When Grand Wash spilled over to Gregg basin, progradation from the south was diminished, which allowed local sediment from the closer provenance of Wheeler Ridge to advance southward into Gregg and Temple basins. Alternatively, Gregg and Temple basin were derived from a different provenance than Grand Wash Trough throughout their deposition. The absence of grains younger than 235 Ma in Gregg-Temple basins suggests that none of the Hualapai basins was receiving sand from the Colorado River until post-Hualapai time. The Pliocene Colorado River samples jointly contain 21% grains younger than 215 Ma, and the modern Colorado River sands jointly contain 12% grains younger than 230 Ma. The combined data suggest that Grand Wash basin was internally drained from 25 to ca. 7 Ma. This expands the time frame of the Muddy Creek constraint (Lucchitta, 2013) during which Grand Wash Trough was receiving only local detritus prior to the arrival of the Colorado River 5–6 Ma (Lucchitta, 1966, 2013; Beard, 1996; Pederson, 2008). These detrital-zircon data are less consistent with a proposed proto–western Grand Canyon (Young, 2008; Wernicke, 2011; Flowers and Farley, 2012; Hill

and Polyak, 2010, 2014) because such a paleocanyon-paleoriver system should have conveyed Paleozoic detritus from its canyon walls to Grand Wash Trough. Thus, both the geochemical and detrital-zircon data support a model for hydrochemically and depositionally separate, internally drained, fault-bounded basins prior to ca. 6 Ma (Spencer et al., 2013; Faulds et al., 2001) in which the lake/marsh water came dominantly from Colorado Plateau groundwater, but the sediment came from local fault blocks to the south and west.

New Isotopic and Chemostratigraphic Data

Geochemical analyses of Hualapai Limestone were also conducted to evaluate chemostratigraphy within and between individual basins. As noted by other authors (Faulds et al., 2001; Wallace et al., 2005; Spencer et al., 2001), the general absence of evaporite facies between 12 and 6 Ma (except at the base) suggests persistent throughput of water in all three lake/marsh basins during carbonate deposition. Thus, the chemostratigraphy can reveal the nature of waters and temporal trends in water chemistry during this extended 12–6 Ma time interval.

Figure 10 shows up-section variation in $^{87}Sr/^{86}Sr$, $\delta^{18}O$, and $\delta^{13}C$. In our best-constrained section (eastern Grand Wash section; black squares), $^{87}Sr/^{86}Sr$ is fairly consistent (~0.719) from the base to ~60 m below the top, and then it decreases up section to values of 0.711. This is similar in the other Grand Wash section (yellow squares). Gregg basin and Temple basin show $^{87}Sr/^{86}Sr$ values of ~0.713–0.715 with no marked up-section variation. In $\delta^{18}O$, Grand Wash basins (black, purple, yellow squares) and especially the eastern Grand Wash section (black) show an initial change to more negative (lighter) $\delta^{18}O$ starting about –60 m and then a shift toward heavier $\delta^{18}O$ in the upper 20 m. Gregg basin (orange circles) is similar and shows an increase in variability and a trend toward heavier $\delta^{18}O$ in the upper 50 m, especially in the Hualapai Wash section. Temple basin shows fairly uniform $\delta^{18}O$. There are similar stratigraphic trends in $\delta^{13}C$. Grand Wash basin, and especially in the eastern Grand Wash measured section, shows increasingly negative $\delta^{13}C$ values up section starting at ~60 m from the top. Gregg basin shows this same trend, but perhaps starting ~80 m from the top. Temple basin also shows lighter $\delta^{13}C$ up section in the upper ~25 m.

The $\delta^{18}O$ and $\delta^{13}C$ stable isotopic values are fairly constant in the lower 150 m of the Grand Wash basin (perhaps 12 to ca. 8 Ma), whereas isotopic character changes, and higher variability is seen in the upper ~50 m. We interpret these up-section trends to mean that the Grand

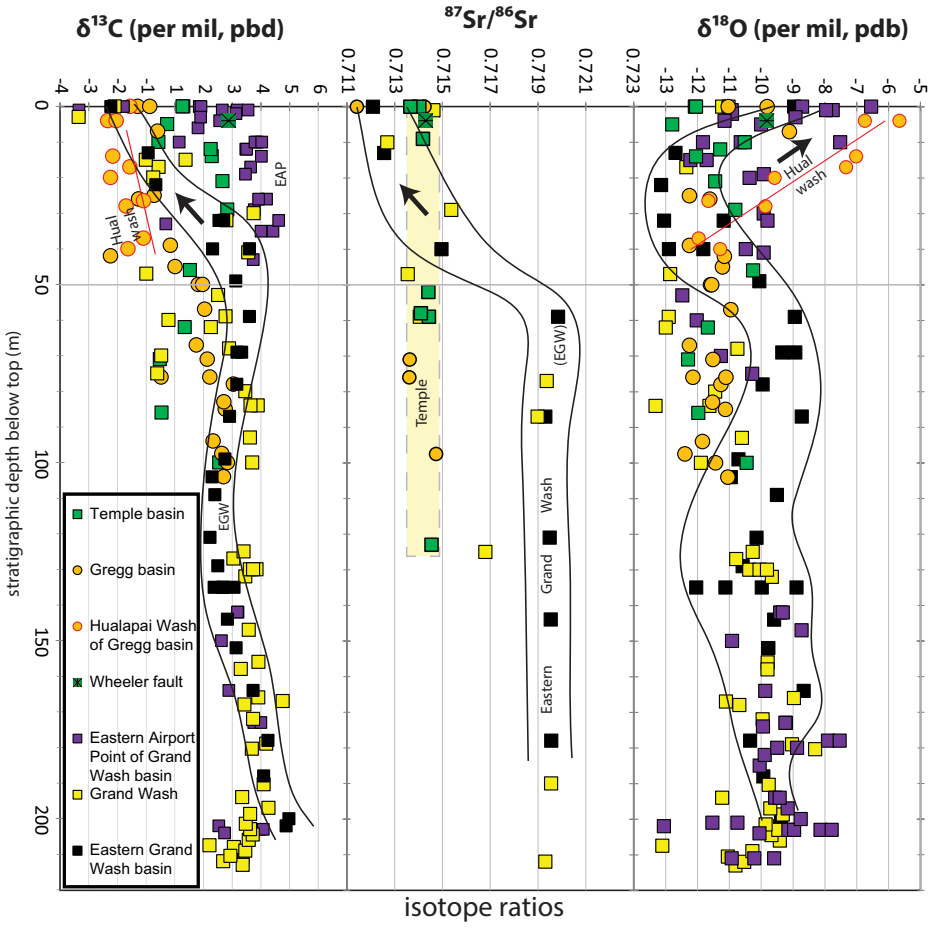

Figure 10. Chemostratigraphy of the Hualapai Limestone by basin shows up-section decrease in $^{87}Sr/^{86}Sr$ (center column) in the upper ~60 m; this is interpreted to record freshening of Grand Wash basin lake waters by input of less-radiogenic Colorado Plateau groundwater before integration of the Colorado River through Grand Canyon. The $\delta^{18}O$ values (right column) show lighter values in the eastern Grand Wash measured section (black squares) starting at ~50 m below the top, which is also consistent with a freshening at ca. 7–8 Ma due to increased throughput of high-elevation recharge. This was followed by an increase in $\delta^{18}O$ (heavier values), interpreted as due to increased evaporation due to lake expansion and spillover at ca. 6–7 Ma. The $\delta^{13}C$ values show up-section decrease (lighter values) in both eastern Grand Wash and Gregg basins starting in the upper ~75 m; this is interpreted to reflect freshening by increased proportions of Colorado River water relative to degassed carbonic groundwater in the past ca. 6–7 Ma.

Wash basin received progressively more meteoric input (hence lower $^{87}Sr/^{86}Sr$) during deposition of the upper ~50 m of the section, likely corresponding to the time interval from ca. 8 to 6 Ma. The change toward more negative $\delta^{18}O$ and more negative $\delta^{13}C$ that takes place at about the same stratigraphic level (–60 m) in multiple sections is also consistent with freshening of lake/marsh waters, because lighter $\delta^{18}O$ is consistent with addition of high-elevation Colorado Plateau recharge, and lighter $\delta^{13}C$ is consistent with more open-system behavior (Talbot, 1990). The change toward heavier $\delta^{18}O$ in the uppermost tens of meters of the eastern Grand Wash and Hualapai Wash sections is consistent with increased evaporation due to higher lake levels during integration of the basins.

Figure 11 is a plot of $\delta^{13}C$ versus $\delta^{18}O$ for the different basins of the Hualapai Limestone. Grand Wash basin $\delta^{18}O$ and $\delta^{13}C$ values overlap strongly with modern travertines being deposited by Havasu Spring (O'Brien et al., 2006), and they are similar to a western Grand Canyon speleothem sampled near Rampart Cave. The different subbasins of the Hualapai Limestone overlap but have somewhat different stable isotope signatures, as discussed in the following. A new data set from northern Grand Wash Trough

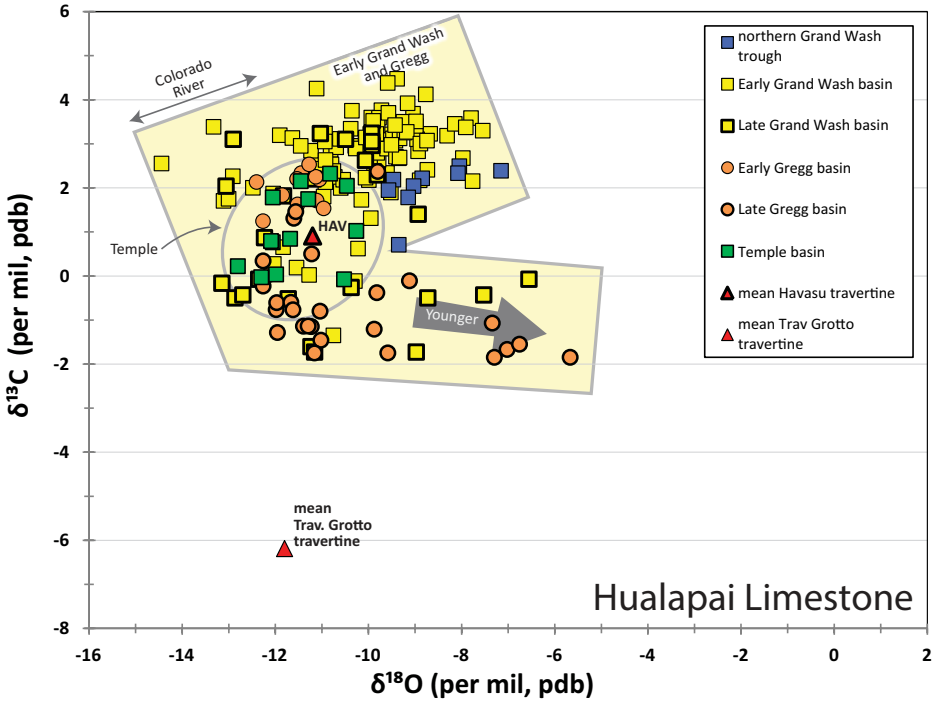

Figure 11. $\delta^{13}C$ vs. $\delta^{18}O$ plot of the Hualapai Limestone by basin (pdb—Peedee belemnite). Older parts of Grand Wash and Gregg basins show strong overlap with Havasu travertine (HAV; red triangle) suggesting derivation of Hualapai Limestone from western Colorado Plateau groundwaters. Hydrochemical changes in the upper parts of the Grand Wash and Gregg basins toward more positive $\delta^{18}O$ (black arrow) are interpreted to be due to spillover and increased evaporation during downward integration. Temple basin shows less variability and overlaps with both Grand Wash and Temple basin and is interpreted to represent well-mixed Hualapai Limestone waters achieved during downward integration.

(blue symbols in Fig. 11) overlaps with that of southern Grand Wash Trough and suggests they may have been part of the same or similar lake/marsh system formed between the Grand Wash and Wheeler faults.

The $^{87}Sr/^{86}Sr$ range for Grand Canyon travertines (0.7099–0.7195) is also similar to the Hualapai Limestone (0.7114–0.7195). Stable isotope and $^{87}Sr/^{86}Sr$ values differ markedly from values of the modern Colorado River near Lake Mead ($^{87}Sr/^{86}Sr$ of 0.7098–0.7108, $\delta^{18}O$ ~−13‰). We conclude that, prior to ca. 8 Ma, Hualapai Limestone precipitated from Colorado Plateau groundwaters similar to those in western Grand Canyon. However, after ca. 8 Ma, Hualapai Limestone deposition reflects increased proportions of higher-elevation Colorado Plateau groundwater. Both source waters were quite distinct from Colorado River water. The marked difference in both $^{87}Sr/^{86}Sr$ and stable isotope composition between Colorado River water and Hualapai Limestone argues against models for infiltration and piping or syphoning of paleo–Colorado River water through caves and sinkholes as a major step in integration of the Colorado River across the Kaibab uplift and through Grand Canyon (Hunt, 1956; Hill et al., 2008; Hill and Polyak, 2010, 2014; Pederson, 2008).

We conclude that the Hualapai Limestone of Grand Wash subbasin was a spring-fed lacustrine system that, especially in its upper ~50 m, records evolving regional groundwater flow paths from the Colorado Plateau. Grand Wash, Gregg, and Temple basins have subtle differences, yet they are similar enough that we postulate partial hydrochemical connectedness in the 1–2 Ma leading up to integration of the basins. The variability of Grand Wash and Gregg basin waters suggests poorly mixed waters (spatially and/or temporally), and less variability in Temple basin suggests better mixed waters. By ca. 6 Ma (–50 m in Temple basin section), the similarity of isotopic trends and values in all three basins is compatible with an interpretation that hydrochemical integration had been established. The observed gradual chemostratigraphic changes over the million-year time scale are not well explained by lake spillover models for an abrupt freshening of Lake Hualapai (Scarborough, 2001).

The discovery of meter-scale rimstone dams at the divide between Grand Wash and Gregg basins at western Airport Point (Fig. 12A) provides evidence for meter-scale surface-water flow depth and water turbulence to allow degassing of carbonic waters. The scale of the rimstone dams is similar to structures seen in Havasu Creek (Fig. 12B). Sr data reveal values of ~0.713–0.715 in the thickest part of the carbonate section, in travertine veins along the Wheeler fault, and for some samples near the top of the section near the pour-over divide. However, samples in adjacent measured sections (Hualapai Wash vs. Spring Wash) show widely disparate values of ~0.7114 and 0.7195 (respectively). This variation near the top of the Gregg basin sections may record the mixing of spillover waters (from Grand Wash basin; 0.712) with fault- derived spring waters along the Wheeler fault (0.714), and still more radiogenic spring waters from the Wheeler fault (up to 0.7195) that are similar to springs in modern western Grand Canyon. The $\delta^{18}O$ and $\delta^{13}C$ values in Gregg basin show hydrochemical separation from Grand Wash values in upper parts of the carbonate section, with the heavier $\delta^{18}O$ waters interpreted to record increased evaporation as lake surface area increased. More homogenized waters in Temple basin may suggest integration of all three basins by ca. 6 Ma. The combined data are compatible with models proposing partially disconnected hydrologic basins, each characterized by different $\delta^{18}O$-$\delta^{13}C$ mixing arrays before 6 Ma, that became integrated across a local spillover path between the two basins near the end of Hualapai Limestone deposition during downward integration (Blackwelder, 1934; House, et al., 2008; Spencer et al., 2013).

Temple basin (Mine Road section of Pearce, 2010) contains the location of the 5.97 Ma ash (Spencer et al., 2001) used for the age of the upper Hualapai Limestone. This section overlies evaporates, and the carbonates may be younger than those of other basins (Roskowski et al., 2010). Chemostratigraphy (Fig. 9) shows little variation in $\delta^{18}O$ and an up-section 2‰ increase in $\delta^{13}C$ at the top of the section. The combined lower variability of $\delta^{18}O$, $\delta^{13}C$, and $^{87}Sr/^{86}Sr$ data suggests that this basin was relatively well mixed during Temple basin time, compared to other basins, perhaps suggesting a shorter history of deposition here that was more narrowly linked in time to the integration event.

BOUSE FORMATION

Overview

The Bouse Formation of the Lower Colorado River region (Metzger, 1968) consists of a thin basal carbonate (meter to decimeter scale) that

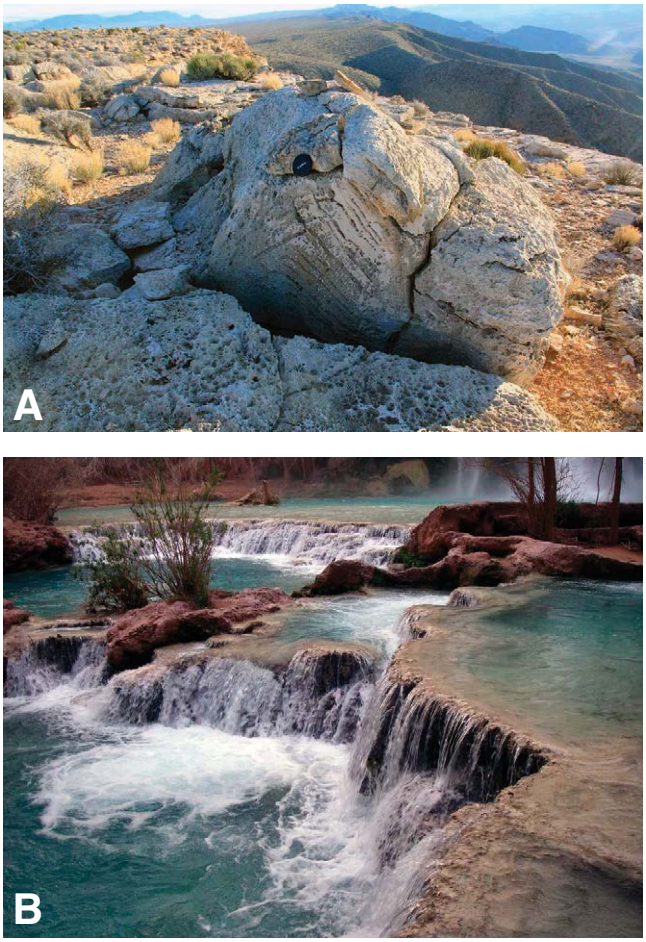

Figure 12. (A) Rimstone paleodams at the spillover divide between Grand Wash and Gregg basins near South Cove; flow was to the right (west). (B) Similar-scale rimstone dams in modern Havasu Creek formed by degassing of CO_2-rich waters and consequent precipitation of travertine at the lip of dams.

overlies Miocene fanglomerates and in turn is overlain by up to ~230 m of siliciclastic claystone, mudstone, and sandstone. The basal carbonate is interpreted to record first arrival of Colorado River waters, and the siliciclastic deposits are interpreted to record arrival of Colorado River sediment in a delta that prograded into the lacustrine (Spencer et al., 2008, 2013; Pearthree and House, 2014) and/or perhaps intermittently marine basins (Buising, 1990; McDougall and Miranda Martinez, 2014). The Bouse Formation was deposited in several basins: Las Vegas, Cottonwood, Mojave, Havasu, Bristol, northern Blythe (Parker), southern Blythe, and Yuma basins (Figs. 1 and 2; Spencer et al., 2013). Bouse Limestone is geochemically different than Hualapai Limestone in terms of its $^{87}Sr/^{86}Sr$ (Fig. 2), and each basin has subtle differences that reflect their own local hydrochemical settings. The age of the Bouse Formation is constrained to be younger than the 5.6–5.84 Ma tuff of Wolverine Creek that underlies it in the Mojave basin, and it is directly dated at 4.83 ± 0.01 Ma by the age of interbedded tuffs in Bristol basin (Harvey, 2014). Dorsey et al. (2007, 2011) concluded that Colorado River sediment first arrived in the Salton Trough at Split Mountain Gorge (location SM, restored in Fig. 1) at 5.3 Ma.

The thin basal Bouse carbonate rests on older fanglomerates across a wide range of elevations within individual basins, and it is interpreted to be a depositional drape that formed as the lakes quickly filled (e.g., House et al., 2008; Spencer et al., 2008, 2013). Elevations of the highest outcrops are interpreted to record lake highstands, which differ from lake to lake across bedrock divides as shown in Figure 1 and the inset to Figure 2: (1) Las Vegas basin (650 m), with divides at upper Black Canyon and modern-day Hoover Dam, (2) Cottonwood basin (560 m) extending to the Pyramid divide (Pearthree and House, 2014), (3) Mojave basin (560 m) extending south to Topoc divide, (4) Havasu basin (360 m) extending to a divide at Parker; (5) Bristol basin (330 m), a NW arm of Blythe basin (Spencer et al., 2013; Miller et al., 2014), and Blythe basin (330 m), which extended to the Chocolate Mountains divide; and (6) Yuma basin, where the top of the inferred Bouse Formation is as much as 1 km below sea level (Olmsted et al., 1973). The Imperial Formation (Fish Creek–Vallecito basin and SM in Fig. 1) was deposited in the northern Gulf of California and is restored by ~230 km of slip across the San Andreas fault system to its approximate 5–6 Ma position. Similarly, the Ridge basin is restored to its original position near the modern Salton Sea. This offset estimate assumes an average slip rate of 45 km/Ma from 5.3 Ma to the present, as indicated by global positioning system (GPS) velocities and geology-based reconstructions (Oskin and Stock, 2003; Plattner et al., 2007; Darin and Dorsey, 2013).

There are alternatives and cautions to the currently popular interpretation that the elevation of Bouse carbonate outcrops reflects a nearly synchronous bathtub-like carbonate lake coating and that the highest outcrops represent relict lake highstands (e.g., Spencer et al., 2013; Pearthree and House, 2014). First, the age and duration of Bouse deposition in different depocenters are incompletely known. Second, simple calculations based on measurements of possible annual varves in Bouse marl suggest that Bouse deposition could have lasted anywhere from 10 to 300 ka (Homan and Dorsey, 2013). Third, there is well-documented post-Bouse movement on some basin-bounding faults at the divides (Miller et al., 2014; Seixas et al., 2015) and within Bouse basins (Metzger et al., 1973; Miller et al., 2014), suggesting that the original extent and distribution of lakes cannot be precisely reconstructed by contouring the modern elevation of the highest Bouse outcrops (Fig. 1). The amount of post-Bouse offset on faults and related changes in elevation remain undocumented and untested.

In the following sections, we combine results of new analyses with published data for multiple tracers ($^{87}Sr/^{86}Sr$, [Sr], $\delta^{13}C$, and $\delta^{18}O$) and apply them to Bouse carbonates to test the similarity or difference between basins. The $^{87}Sr/^{86}Sr$ data are discussed first because of their importance in overturning (Spencer and Patchett, 1997) earlier marine models for parts of the Bouse Formation (Lucchitta, 1979; Buising, 1990).

$^{87}Sr/^{86}Sr$ Isotopic Data

Bouse $^{87}Sr/^{86}Sr$ ratios range from 0.713 to 0.720 (Fig. 2). Each basin has internal variation of ~0.001–0.002, suggesting incomplete mixing within each lake. Most Bouse basins are similar in their variability to, for example, the Lake Bonneville system (0.7115–0.7124; Hart et al., 2004). The range and values of $^{87}Sr/^{86}Sr$ differ subtly but perhaps significantly between basins. For example, Sr isotope ratios in Frenchman Mountain carbonates of the Las Vegas basin (Roskowski et al., 2010) are higher than those of Colorado River water (Gross et al., 2001)

but similar to the range seen in Lake Mead spring waters (Supplemental Table 1 [see footnote 1]), and they may have been elevated by nearby radiogenic springs (Fig. 2). Lake-margin travertines near the highstand of Cottonwood basin (new data) are significantly more radiogenic than basin-center carbonates (Roskowski et al., 2010), suggesting spring inputs. Amboy outcrops are more radiogenic than most Bouse carbonates, also suggesting spring inputs in different subbasins.

Where measured sections in individual locations are available (Blythe, Amboy, Frenchman Mountain), there is no observed up-section change in $^{87}Sr/^{86}Sr$ (thickest section is ~25 m), suggesting rapid deposition. Where samples are available from elevation transects that may record lake filling of a single basin, Blythe basin shows no relationship between $^{87}Sr/^{86}Sr$ and elevation (Roskowski et al., 2010), whereas Mojave basin, like Cottonwood basin, shows a slight increase in $^{87}Sr/^{86}Sr$ at higher elevation. Regionally, the maximum $^{87}Sr/^{86}Sr$ value in each basin decreases to the south (by ~0.0003 per basin), suggesting a southward increase of low-$^{87}Sr/^{86}Sr$ waters (e.g., compatible with increased Colorado River input). All values are higher than marine values, although secondary carbonates within the Bouse Formation of southern Blythe basin (Spencer and Patchett, 1997) are intermediate between marine and marl values (Fig. 2). Marine values of 0.709 were measured in shells from a unit correlated as Bouse Formation in the subsurface of the Yuma basin south of the Chocolate Mountains divide (Eberly and Stanley, 1978). With this one exception, all Bouse carbonates are more radiogenic than modern Colorado River water, and most are more radiogenic than the <10 ka Lake Cahuilla tufas that were fed by the ancestral Colorado River (Li et al., 2008a). Thus, we infer that Colorado River water likely mixed with higher-$^{87}Sr/^{86}Sr$ Lake Hualapai water to produce Bouse waters.

Modeling of $^{87}Sr/^{86}Sr$ and [Sr]

Although $^{87}Sr/^{86}Sr$ values have figured prominently in studies concluding that the Hualapai Limestone and much of the Bouse Formation are nonmarine (e.g., Spencer and Patchett, 1997), no study has yet considered the importance of strontium concentration [Sr] in mixing models. Figure 13A shows the wide range of $^{87}Sr/^{86}Sr$ and [Sr] in waters (small symbols) and carbonates (large symbols) of the lower Colorado River region. Colorado River water [Sr] averages ~1 ppm in eastern Grand Canyon and reaches ~1.2 ppm in Lake Mead. Grand Canyon springs average ~0.5 ppm; Lake Mead area springs average ~3.7 ppm. Evaporative lake waters can have similar [Sr] to the mean of river inflow (e.g., 1.6 and 2.0 ppm for Great Salt Lake and river values, respectively; Hart et al., 2004). However, there is often significant [Sr] enrichment in some saline lakes, for example, ~24 ppm for modern Salton Sea water, which formed in 1905 when Colorado River water with a mean river input = 2.7 ppm entered the basin (Li et al., 2008b). Geothermal spring inputs also can have very high [Sr]: ~600 ppm in the Salton Sea

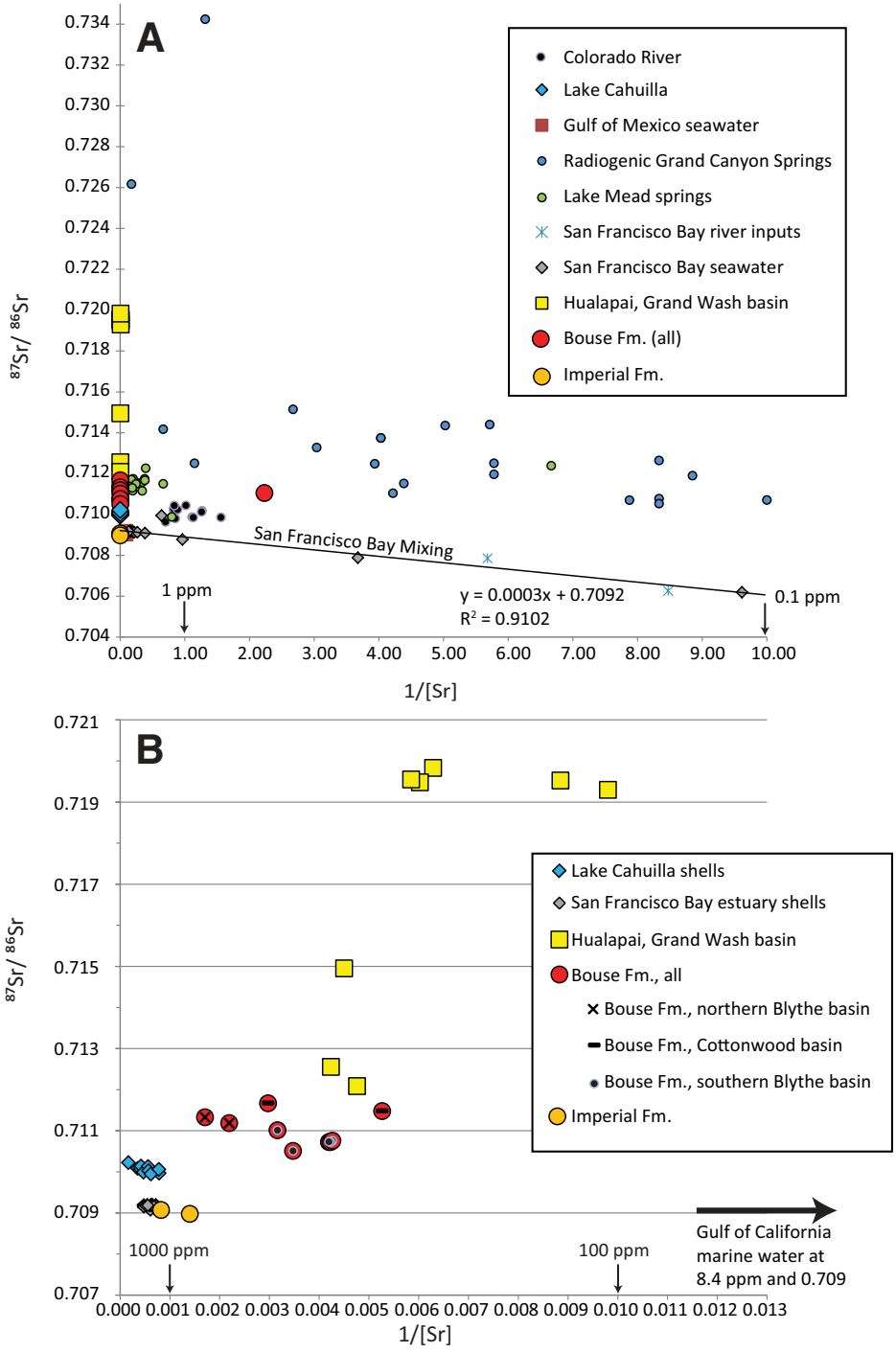

Figure 13. (A) Plot of $^{87}Sr/^{86}Sr$ vs. [Sr] showing large variation due to mixing for Colorado River region waters and carbonates. (B) Close-up of the 100–1000 ppm [Sr] carbonates in the Hualapai Limestone and Bouse Formation showing overall north-to-south decrease in $^{87}Sr/^{86}Sr$ and increase in [Sr] from Hualapai to Bouse. Carbonates (shells) from Holocene Lake Cahuilla and modern San Francisco Bay estuary are shown for comparison.

(Doe et al., 1966). Carbonates that form from saline lake waters can be significantly enriched in [Sr]; for example, Lake Cahuilla tufas that were deposited between 400 and 20 ka by waters dominated by Colorado River input have a mean of ~2300 ppm, with shells approaching [Sr] = 6000 ppm (Li et al., 2008b). The modern Gulf of California seawater has [Sr] = 8.4 ppm; San Francisco Bay marine-estuary waters are variable with mean [Sr] = ~4 ppm (Ingram and DePaolo, 1993). Mean [Sr] for Hualapai Limestone is ~170 ppm; mean [Sr] for Bouse Formation marls is ~400 ppm, and mean [Sr] for Bouse shells is ~900 ppm. Figure 13B shows a north to south decrease in $^{87}Sr/^{86}Sr$ and increase in [Sr] from Hualapai to Bouse basins.

Figure 14 is the first published effort to model the variability of $^{87}Sr/^{86}Sr$ values within and between basins and the importance of [Sr] in determining the mixing proportions needed to explain the observed $^{87}Sr/^{86}Sr$ of different parts of the system. The *y* axis shows the extreme $^{87}Sr/^{86}Sr$ variability (0.008) in the Hualapai Limestone and more limited variability in the Bouse Formation (~0.0015). The *x* axis is the fraction of the more radiogenic end member for a suite of mixing models. Note that mixing of waters with the same [Sr] (1:1) gives linear mixing, whereas mixing end members with variable [Sr] produces curved models. However, [Sr] is unknown for the waters that deposited past carbonates, so Figure 14 models observed $^{87}Sr/^{86}Sr$ in terms of different [Sr] assumptions based on end-member values from our data. This provides a speculative, plausible set of mixing models that could be related to downward integration of the early Colorado River, as follows (numbers are keyed to Fig. 14).

(1) Early Hualapai water: We use a spring end-member $^{87}Sr/^{86}Sr$ value of 0.720 (not our extreme value of 0.735 of western Grand Canyon) to postulate the spring-fed nature of the Grand Wash basin lake/marsh and to explain the fairly consistent values of 0.7193–0.7198 in the early part of the Hualapai Limestone in Grand Wash basin (box 1 of Fig. 14).

(2) Late Hualapai water: Early Hualapai lake/marsh waters are modeled to have mixed with increasing proportions of Colorado Plateau groundwater (CPGW of Fig. 14 with $^{87}Sr/^{86}Sr$ = 0.712), including an increased component of high-elevation recharge to explain the more negative $\delta^{13}O$ in the upper part of the section (Fig. 10). This end member is similar to the mean value of Grand Canyon springs ($^{87}Sr/^{86}Sr$ = 0.7122; [Sr] = 2.6 ppm) and to the high-volume Havasu spring ($^{87}Sr/^{86}Sr$ = 0.7116). This mixing could explain the variability and progressive freshening of $^{87}Sr/^{86}Sr$ observed in the upper 50 m of the Hualapai Limestone ($^{87}Sr/^{86}Sr$ = 0.715–0.712, represented by 2A to 2B in Fig. 13) in terms of the arrival of increasing amounts of Colorado Plateau groundwater. [Sr] for Hualapai-depositing waters is unknown, but we note that the carbonates deposited in early versus later Hualapai Limestone of Grand Wash basin have similar [Sr] (150 vs. 220 ppm, respectively), so we favor a near 1:1 [Sr] ratio mixing model. In the 1:1 model, 2A values would be explained by ~40% early Hualapai water mixing with 60% arriving Colorado Plateau groundwater and 2B by ~10% early Hualapai water mixing with 90% arriving Colorado Plateau groundwater at the very top of the section. Alternatively, if [Sr] values in the early Grand Wash lake/marsh were 4–10 times higher than arriving groundwater, for example, due to evaporative concentration (Li et al., 2008b), a mix of 5%–15% early Hualapai water and 85%–95% Colorado Plateau groundwater would be needed to explain late Hualapai $^{87}Sr/^{86}Sr$ values of 0.712–0.715 (2C in Fig. 14).

Similar models using arriving Colorado River values of 0.710 (and [Sr] = 1–2 ppm) might also explain the progressive change in the upper 50 m of the section toward decreasing $^{87}Sr/^{86}Sr$ and increasing [Sr] in the carbonates. However, the gradual change in the top 50 m of the Grand Wash sections suggests a change over several million years, which is more consistent with the interpretation that the arrival of Colorado

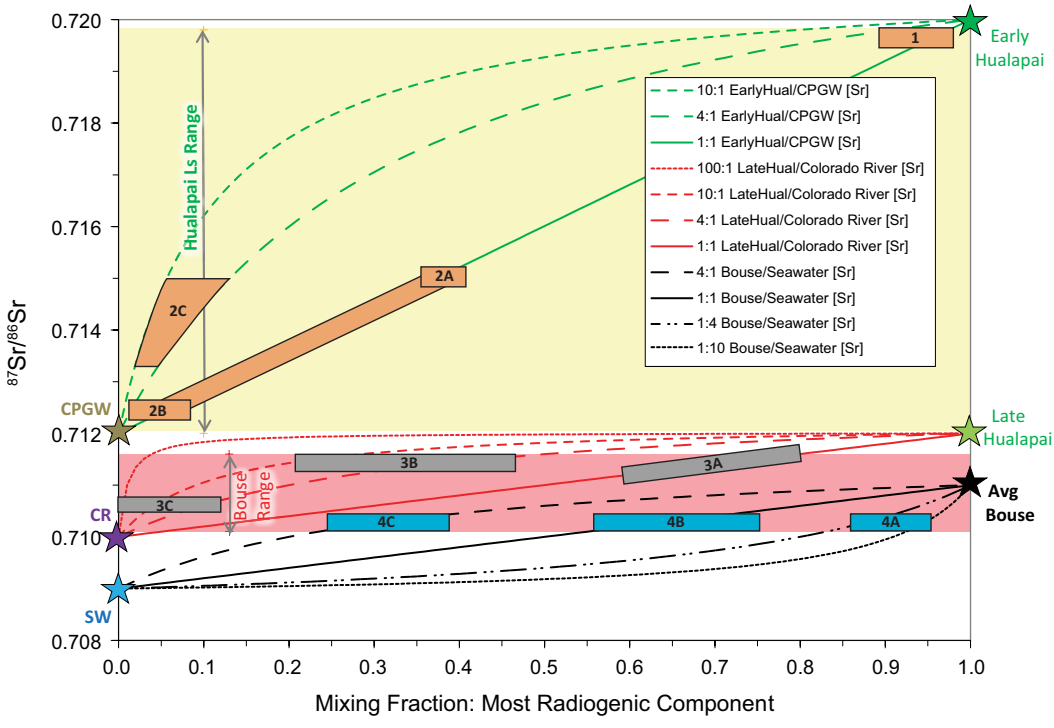

Figure 14. Plot of $^{87}Sr/^{86}Sr$ vs. mixing fraction for a variety of possible end-member [Sr] water values. Simple binary mixing curves and empirically derived "end members" are compatible with the following mixing: 1—early Hualapai Limestone water was sourced from western Grand Canyon springs with $^{87}Sr/^{86}Sr$ = 0.720; 2—early Hualapai waters modeled to have mixed with freshening Colorado Plateau groundwater (CPGW) similar to Havasu spring karst aquifer water to produce the variation in $^{87}Sr/^{86}Sr$ seen in late Hualapai limestones (2A to 2C show results using different [Sr] assumptions); 3—downward integration of late Hualapai water modeled to have mixed with first-arriving Colorado River water (CR) to produce the variability seen in Bouse basins (3A–3C); 4—average Bouse waters modeled to have mixed with increasing components of Colorado River water in a series of open lake systems, followed by covariation of $\delta^{13}C$ and $\delta^{18}O$ along a positive slope compatible with evaporation and/or mixing with seawater (SW) in the southernmost Blythe basin.

Plateau groundwater (rather than the Colorado River) led to downward integration from Grand Wash basin to Gregg and Temple basins.

The ranges of $^{87}Sr/^{86}Sr$ in Gregg and Temple basins (~0.715–0.0711) are not as large as Grand Wash basin, but they are large enough to suggest incomplete mixing in the lakes/marsh systems; we use a value of 0.712 as a reasonable latest Hualapai Limestone value based on the up-section decrease in $^{87}Sr/^{86}Sr$ in all basins (Fig. 10). In 2B and 2C, the large proportion of arriving fresher groundwater suggests that groundwater sapping (Pederson, 2001) may have played a significant role in focusing erosion near springs and led to the integration of the Colorado River across upstream drainage divides and through existing paleocanyon segments to instigate downward integration of Hualapai Limestone basins (Karlstrom et al., 2014).

(3) Bouse Water and arrival of the Colorado River ($^{87}Sr/^{86}Sr$ = 0.710): We model the first arrival of far-traveled Colorado River water (as opposed to Colorado Plateau groundwater) to have mixed with late Hualapai water (~0.712) at 6–5 Ma to produce a few values of 0.712–0.711 in the uppermost Hualapai Limestone and to have initiated downward integration from Temple basin to the Cottonwood basin of the Bouse Formation (Fig. 1; $^{87}Sr/^{86}Sr$ values of 0.7115–0.7117; 3A in Fig. 14). Strontium concentration in the waters is unknown, but Figure 14 shows that if [Sr] concentrations in Temple basin waters were subequal to [Sr] in the Colorado River (1–2 ppm), addition of a relative proportion of 20%–40% Colorado River water with 60%–80% late Hualapai water could produce the Cottonwood basin values (3A of Fig. 14). More likely, based on modern compositions, [Sr] in the arriving Colorado River water would have been 4–10 times lower than late Hualapai water such that the mixture may have been 20%–45% late Hualapai water mixing with 55%–80% Colorado River (3B of Fig. 14). These models are compatible with the notion that a major water-delivery event of Colorado River water (up to 80% of the total water) initiated downward integration of the Hualapai basin to Bouse subbasins (Fig. 1). Increasing proportions of newly arriving Colorado River water during a sequence of lake filling and overflow events may explain the progressive decrease in maximum $^{87}Sr/^{86}Sr$ values downstream in the Bouse basins, for example, a mean of ~0.7108 for Mojave basin (3C of Fig. 14). The models suggest that the range of Bouse $^{87}Sr/^{86}Sr$ values (0.710–0.7115) can be explained by progressively increased proportions of Colorado River water that mixed with Hualapai basin waters during southward-migrating integration of Bouse basins.

(4) Possible marine mixing in Blythe basin (southern Bouse Formation): In this section, we define "Bouse water" as a mixture of first-arriving Colorado River water and older Hualapai basin waters, in which the relative proportion of the two components was rapidly evolving and highly variable in space and time. Previous workers have stressed that $^{87}Sr/^{86}Sr$ ratios in carbonates of the southern Blythe basin (0.710–0.711) are significantly more radiogenic than seawater (0.709) and therefore refute a marine influence on Bouse depositional environments (Spencer and Patchett, 1997; Roskowski et al., 2010). To address this question, model 4 in Figure 14 explores the possibility that $^{87}Sr/^{86}Sr$ ratios in Bouse carbonates could reflect mixing of "Bouse waters" with seawater in a marine-estuary environment (Crossey et al., 2011; McDougall Miranda Martinez, 2014; Miller et al., 2014). If [Sr] in the arriving Bouse water was significantly lower than seawater (~1–2 ppm for Bouse water, compared to 8 ppm for seawater), a mixture with 85%–95% Bouse water and 5%–15% seawater would produce the observed southern Bouse values of 0.710–0.711 (4A, Fig. 14). If [Sr] of the arriving Bouse water was subequal to that of seawater (~8 ppm), the observed Sr isotopic ratios could be produced with a mixture of 55%–75% Bouse water and 25%–45% seawater (4B of Fig. 14). If [Sr] in the arriving Bouse water was ~4 times higher than seawater, a mixture of 25%–40% Bouse water with 60%–75% seawater would produce the Sr isotopic ratios observed in Bouse carbonates (4C of Fig. 14).

Thus, for the southernmost Blythe basin where marine fossils are present, the elevated Bouse $^{87}Sr/^{86}Sr$ values (0.710–0.711) relative to seawater (0.709) can plausibly be explained with ~5%–50% seawater mixed with arriving Bouse water (itself a mixture of earliest Colorado River water and older Hualapai basin waters). This modeling indicates that it is neither difficult nor implausible to generate radiogenic values of 0.710 in a Bouse Formation marine-estuary system, contrary to the assertions of previous studies (Spencer and Patchett, 1997; Roskowski et al., 2010; Spencer et al., 2008, 2013). Our mixing models are essentially a "reverse analog" of the modern San Francisco Bay estuary, where waters of the arriving Sacramento and San Joaquin Rivers are much less radiogenic ($^{87}Sr/^{86}Sr$ = 0.7065; [Sr] = 0.13 ppm) and mix with seawater ($^{87}Sr/^{86}Sr$ = 0.7092; [Sr] = 7.9 ppm) in the estuary to produce surface-water values in the estuary that show a wide spread of $^{87}Sr/^{86}Sr$ values (Fig. 2). This variation was interpreted by Ingram and Sloan (1992) to reflect density stratification as well as seasonal and millennial changes in runoff into the San Francisco Bay. A next step in evaluating this hypothesis for the Bouse Formation is to reconcile the diversity of planktic foraminifers (McDougall and Miranda Martinez, 2014) with possible mixtures of marine and Bouse waters, resulting salinities, and information from other chemical tracers.

In addition to mixing between Bouse waters and seawater, input of endogenic and geothermal groundwaters could also have exerted an important influence on elevated Sr isotopic ratios (Crossey et al., 2011). For example, Salton Sea geothermal sites have $^{87}Sr/^{86}Sr$ = 0.7110–0.7115, and [Sr] is up to 600–900 ppm (Doe et al., 1966), indicating that geothermal brines could have played a role in mixing. Shallow groundwater in the Imperial Valley is predominantly from the Colorado River, but mixing is seen between these waters and geothermal brines in the Salton Sea region, and seawater mixing with groundwater is documented in coastal springs in Baja, California (Coplen and Kolesar, 1974). In a similar fashion, geothermal groundwaters with high $^{87}Sr/^{86}Sr$ and [Sr] could have had large leverage in mixing with other water sources in the southern Blythe basin (Crossey et al., 2011).

Overall, our models are compatible with Bouse limestones that formed in a mixture of Lake Hualapai water with voluminous first-arriving Colorado River water (in agreement with Spencer et al., 2013) but not by Colorado River water itself (Patchett and Spencer, 2001). Due to a general lack of data on [Sr] composition of the Pliocene lake waters, the models are permissive of alternate hypotheses (Miller et al., 2014): Bristol basin may have been an arm of Lake Blythe with local spring input that explains higher $^{87}Sr/^{86}Sr$, and/or southern Blythe basin could have seen intermittent mixing of marine water (25%–75%) and still deposited carbonates with radiogenic values of 0.710–0.711. Similar mixing models could also be generated that would be compatible with no marine mixing and, instead, an increase in the percentage of Colorado River water through time (Spencer et al., 2013). Thus, our plausibility arguments to try to reconcile Bouse $^{87}Sr/^{86}Sr$, marine paleontology (without reliance on avian transport), and stable isotope data (see following) via an estuarine mixing of nonmarine and marine waters are aimed at focusing additional efforts to test alternative models. Additional $^{87}Sr/^{86}Sr$ analyses, with stratigraphic context, should be focused on outcrops with high diversity of planktic foraminifers below ~110 m elevation (110 m contour of Fig. 1), as well as subsurface Bouse samples (MacDougal and Miranda Martinez, 2014) to continue to look for any $^{87}Sr/^{86}Sr$ values between 0.709 and 0.710. Marine values of 0.709 are found in the subsur-

face of the Yuma basin in rocks correlated with Bouse Formation (Eberly and Stanley [1978] *in* Spencer and Patchett, 1997) indicating that Gulf of California seawater was at least as far north as latitude 32.7°N in the Colorado River deltaic system at ca. 5–6 Ma (Fig. 1).

Stable Isotopes

Figure 15 shows a compilation of new and published $\delta^{18}O$ and $\delta^{13}C$ values for Bouse Formation carbonates, in comparison with stable isotopes of the Hualapai Limestone (yellow shading). Bouse samples are highly variable and fall into several groups, with interesting differences between basins. Working downstream, Cottonwood basin is displaced markedly downward (~4‰ lighter in $\delta^{13}C$ and $\delta^{18}O$) relative to Temple basin and most of the Hualapai Limestone but overlaps with samples from the top of Gregg basin. This is compatible with spillover and downward integration of Gregg basin waters to Temple, and then to Cottonwood basin, with considerable evaporation to explain the ~6‰ heavier $\delta^{18}O$ in Cottonwood basin (2–3 of Fig. 15). Mojave basin displays weak covariance of $\delta^{18}O$ and $\delta^{13}C$ values, which have a similar negative slope to Grand Wash and Gregg basin (interpreted as a spillover trend), and mean values are ~4‰ lighter in $\delta^{18}O$ (3–4 of Fig. 15), compatible with a higher proportion of arriving high-elevation Colorado River recharge during Cottonwood to Mojave spillover (House et al., 2008). Havasu basin values are several per mil heavier in $\delta^{13}C$ (4–5 of Fig. 15), compatible with, for example, CO_2 degassing during spillover, increased residence time, and/or higher primary organic productivity in Lake Havasu (Fig. 3). Blythe basin values overlap with those of the Cottonwood and Mojave basins, but input source waters (lower left of the covariation trend; Talbot, 1990) are heavier in $\delta^{18}O$ (6–7 of Fig. 15), compatible with increased downstream evaporation. Large variation in stable isotopes within basins suggests incomplete mixing. Thus, the overall shift to heavier $\delta^{18}O$ and lighter $\delta^{13}C$ from Hualapai to the southern Blythe basin (schematically shown in Fig. 3) suggests independent variations between isotopic systems, which is common in open, short-residence-time lakes (Talbot and Kelts, 1990).

Figure 16 shows details of $\delta^{18}O$ and $\delta^{13}C$ covariation for the southern Blythe basin. Marls form a linear array (R^2 = 0.66) with a slope similar to the Lake Cahuilla and Great Salt Lake arrays (Fig. 3) and compatible with evaporation. However, this is anchored near (0,0), which is typical of marine estuaries (e.g., San Francisco Bay) but rare in closed lake systems (e.g., Talbot, 1990; Davis et al., 2012). Fossils in the

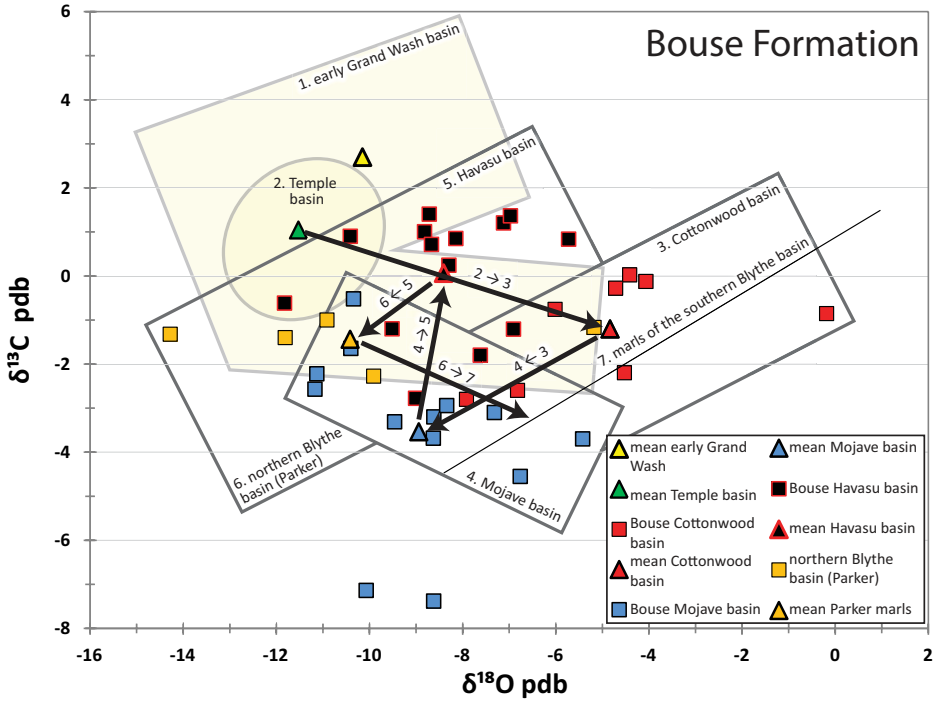

Figure 15. $\delta^{13}C$ vs. $\delta^{18}O$ plot of the Bouse Formation carbonates by basin (pdb—Peedee belemnite). A mix of Havasu Limestone water (light shading) plus first-arriving Colorado River water is interpreted to be the main sources for Bouse waters (2–3 arrow). From north to south: Cottonwood basin $\delta^{13}C$ and $\delta^{18}O$ are similar to upper Hualapai waters and are interpreted to be due to additional evaporation during spillover and downward integration. Mojave basin has lighter $\delta^{18}O$ than Cottonwood, suggesting an increased proportion of arriving Colorado River water (3–4 arrow). Lake Havasu basin has $\delta^{13}C$ and $\delta^{18}O$ values similar to Mojave basin water mixed with additional Colorado River waters (4–5 arrow). Southernmost Blythe basin has heavier $\delta^{18}O$ and lighter $\delta^{13}C$ than other Bouse basins (6–7 arrow) and may represent continued arrival of Colorado River water in an open lake system followed by a positive covariation trend in the marls of southern Blythe basin due to evaporation and/or mixing with seawater.

southern Blythe basin tend to be heavier in $\delta^{13}C$ than the marls and up to 10‰ heavier than San Francisco Bay mussels, reflecting organic fractionation and different mixes of waters (Talbot and Kelts, 1990).

Figure 17 is a plot of $^{87}Sr/^{86}Sr$ versus $\delta^{18}O$. The multitracer approach should be able to produce compatible mixing models for both of these tracers, because both are robust indications of the composition of waters that deposited the carbonates. These data are compatible with the downstream integration sequence described herein for $^{87}Sr/^{86}Sr$, and they provide another way to assess the chemostratigraphy trends in Figure 10, thus providing additional insight to possible extent of evaporation in different parts of the system. With numbers keyed to Figure 17, our interpretation is: (1) The most likely source of early Hualapai waters was groundwater from the western Grand Canyon region, where the most radiogenic springs reach values of $^{87}Sr/^{86}Sr$ = 0.72–0.735, and $\delta^{18}O$ is similar to western Grand Canyon travertines ($\delta^{18}O$ = –9‰ to –11‰) but not to high-elevation recharge or Colorado River water ($\delta^{18}O$ = –12‰). (2) Integration of basins of the Hualapai Limestone system involved progressive freshening of waters due to arrival of Colorado Plateau groundwater with $\delta^{18}O$ = –9‰ to –13‰, dissimilar to Colorado River water at Lees Ferry ($\delta^{18}O$ = –15‰; $^{87}Sr/^{86}Sr$ < 0.7105) but similar to mean Grand Canyon and Lake Mead spring water ($\delta^{18}O$ = –11.5‰; $^{87}Sr/^{86}Sr$ = 0.7124). (3) Arrival of the Colorado River abruptly introduced large volumes of low-$^{87}Sr/^{86}Sr$ and negative-$\delta^{18}O$ water that drove spillover and downward integration of Temple basin water to Bouse basins. Waters became progressively less radiogenic in $^{87}Sr/^{86}Sr$ to the south due to higher proportions of river water during downward integration, but they became heavier in $\delta^{18}O$ due to increased evaporation. The variability of both parameters suggests incomplete mixing in different basins and/or enough time for local fractionation and

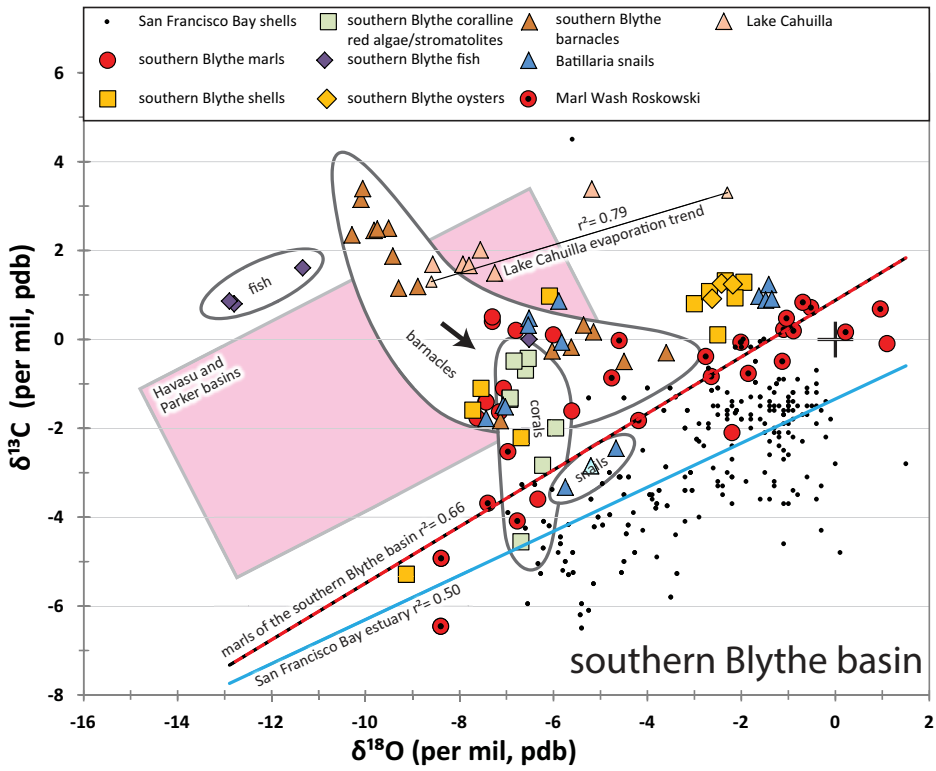

Figure 16. $\delta^{13}C$ vs. $\delta^{18}O$ plot of southern Blythe basin marls and fossils (pdb—Peedee belemnite). Marls show a well-defined $\delta^{13}C$ and $\delta^{18}O$ covariation trend (R^2 = 0.66) that extends from (0,0) to lighter values. This trend is similar to modern San Francisco Bay estuary molluscs and different than most lakes worldwide, including Great Salt Lake and Lake Cahuilla. Many fossils in the southern Bouse basin are heavier in $\delta^{13}C$ than marls due to organic fractionation.

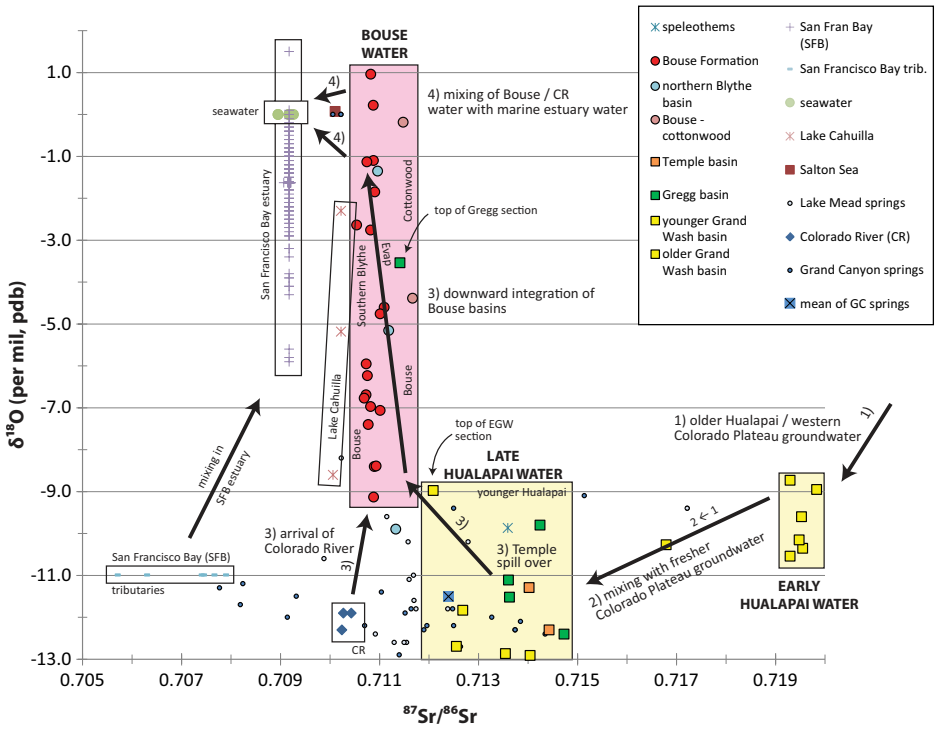

Figure 17. $^{87}Sr/^{86}Sr$ vs. $\delta^{18}O$ for the inferred downward integration of Lake Hualapai basins to-and-through different Bouse basins. As with $^{87}Sr/^{86}Sr$ mixing in Figure 12: 1—western Colorado Plateau groundwaters are inferred as the source of the older parts of the Hualapai Limestone in Grand Wash basin; 2—6–8 Ma input of progressively fresher Colorado Plateau groundwater is inferred to explain the up-section change in Hualapai Limestone observed in the top ~50 m of the section; 3—arrival of the Colorado River ca. 5–6 Ma is interpreted to have caused spillover and downward integration of the Hualapai basins to Bouse basins and a complex southward change in hydrochemistry, with overall trends toward more negative $\delta^{18}O$ values from north to south interpreted as increased proportion of Colorado River water plus evaporation effects; 4—mixing of radiogenic Bouse water with seawater may have taken place in the southernmost Blythe basin in a "reverse analog" to mixing of nonradiogenic tributary waters in the San Francisco Bay estuary system. GC—Grand Canyon; EGW—eastern Grand Wash.

mixing processes to affect Bouse basins differently. (4) At the southern end, a near-seawater $\delta^{18}O = 0‰$ could reflect evaporation in a closed lake system (except note that Lake Cahuilla does not get as heavy in $\delta^{18}O$) and/or mixing of seawater in the southern paleolake Blythe (e.g., Ingram et al., 1996; Sampei et al., 2005; Augley et al., 2007). Similarly, $^{87}Sr/^{86}Sr$ mixing with ~50% seawater could plausibly explain both the $^{87}Sr/^{86}Sr$ and near-zero $\delta^{18}O$ in the southernmost Blythe basin.

DISCUSSION AND CONCLUSIONS

The geochemistry of modern springs in Grand Canyon shows significant variability within a given spring group, with up to 0.02 variation in $^{87}Sr/^{86}Sr$, interpreted to reflect differential mixing of deeply derived (endogenic) fluids with meteoric (epigenic) recharge. The ~2‰–4‰ covarying arrays of $\delta^{13}C$ and $\delta^{18}O$ are interpreted to reflect seasonal fractionation and groundwater mixing. Western Grand Canyon springs have higher $^{87}Sr/^{86}Sr$ ratios (0.710–0.735) relative to eastern springs (0.707–0.715). Quaternary (<1 Ma) travertine and speleothems (2–4 Ma) associated with Grand Canyon springs and groundwaters show ranges of $^{87}Sr/^{86}Sr$, $\delta^{13}C$, and $\delta^{18}O$ in carbonate that overlap with modern water values. These data from young water-carbonate systems provide justification for using carbonate values as a proxy for the water from which they were deposited.

The Hualapai Limestone was deposited from 12 Ma (new ash age) to 6 Ma and is up to 210 m thick. It exhibits variation stratigraphically and between fault-bounded basins. (1) Grand Wash basin has $^{87}Sr/^{86}Sr$, $\delta^{13}C$, and $\delta^{18}O$ values and ranges similar to western Grand Canyon springs and travertines, and we infer that this basin records a spring-fed lake/marsh system sourced in large part by western Colorado Plateau groundwaters. Up-section chemostratigraphic trends suggest a gradual increase (probably over 1–2 Ma) in groundwaters that delivered recharge from higher elevations. A lack of evaporites (after ca. 13 Ma) indicates continuous flow through Grand Wash and Gregg basins, with a flow path postulated to have been focused southwards along the Grand Wash fault to Red Lake evaporite basin. Meter-scale rimstone dams suggest surface flow and lake spillover were active during downward integration to Gregg basin. (2) Gregg basin shows an up-section increase in $\delta^{18}O$ and decrease in $^{87}Sr/^{86}Sr$ and $\delta^{13}C$, which are interpreted to reflect up-section freshening of waters. (3) Temple basin has less pronounced up-section variation in $^{87}Sr/^{86}Sr$, $\delta^{13}C$, and $\delta^{18}O$, suggesting the arrival of combined waters from Hualapai and Gregg basins at ca. 6 Ma. These geochemical data suggest hydrologically distinct basins before ca. 6 Ma. Detrital-zircon spectra from red siltstones underlying the Hualapai Limestone in Grand Wash and Temple basins (Dickinson et al., 2014) also suggest that they were separate basins prior to ca. 6 Ma. We envision a set of fault-segmented internally drained lakes that were integrated ca. 6 Ma to form a single Hualapai lake basin.

We propose that groundwater sapping was an important mechanism for the eventual integration of the Colorado River from the Colorado Plateau to Grand Wash Trough ca. 6 Ma. Groundwater flow and spring discharge can influence erosion and facilitate reorganization of surface-water drainage (Pederson, 2001). Potentially related mechanisms include karst piracy (e.g., transport of Colorado River water through cave passages under the Kaibab uplift; Hill and Polyak, 2014), karst piping (e.g., infiltration of surface water from Hualapai Plateau to Grand Wash through caves; Hunt, 1969; Pederson, 2001), and more general karst connections (where caves connect surface-water drainages beneath a topographic divide; Hill et al., 2008). Our groundwater sapping model does not involve Colorado River surface water moving through caves to explain deposition of the Hualapai Limestone. In contrast to Hunt (1969, 1969), Pederson (2001), and Hill and Polyak (2014), we envision pre–Colorado River movement of groundwater similar to today's Redwall Muav aquifer. Thermochronologic data suggest that the Kaibab uplift had already been breached 25–15 Ma (Lee et al., 2013; Karlstrom et al., 2014). The ensuing 12–6 Ma deposition of Hualapai Limestone is interpreted here in terms of groundwater flow, first from the western Colorado Plateau (highly radiogenic early Hualapai water) and then from higher-elevation Colorado Plateau sources (late Hualapai water). Deposition of the Hualapai Limestone necessitated high-p_{CO_2}, highly radiogenic, and heavy $\delta^{18}O$ waters, very different than the modern Colorado River water. The groundwater sapping mechanism, operating over millions of years (12–6 Ma), could have influenced Grand Wash lake throughput and evolving hydrochemistry, focused springs into existing basins and paleocanyons (Karlstrom et al., 2014), and led to drainage reorganization and eventual integration of the Colorado River in its present path 5–6 Ma. Geochemical data seem best explained by a fairly abrupt arrival of voluminous Colorado River that mixed with late Hualapai water and caused downward propagation of lake basins of the Bouse Formation between 5.8 and 4.8 Ma.

Carbonates of the Bouse Formation (5.8–4.8 Ma) were also deposited in several basins separated by bedrock divides (Fig. 1). The basal carbonate is interpreted to record continued downward integration of the Colorado River in water-delivery events resulting from a combination of groundwater sapping and spillover of higher basins. Upper siliciclastic units of the Bouse Formation contain Colorado River sands, and the unit overall is interpreted (in agreement with models of Spencer et al., 2013) to record a downward-integrating lake system that led to final integration of the Colorado River system to the Gulf of California. Hydrochemical tracers suggest several new aspects to this model: (1) Las Vegas has $^{87}Sr/^{86}Sr$ values compatible with mixing of Hualapai and local spring waters with first-arriving Colorado River water. (2) Cottonwood basin carbonates are more radiogenic (higher $^{87}Sr/^{86}Sr$) than carbonates of Las Vegas basin, suggesting addition of radiogenic spring waters similar to modern hot springs below Hoover Dam. The $\delta^{18}O$ value in Cottonwood basin is similar to that of Gregg basin but heavier than Temple basin carbonates, suggesting that Cottonwood basin carbonates precipitated from Hualapai-like waters that had seen additional evaporation and/or springs inputs. (3) Mojave basin has less radiogenic $^{87}Sr/^{86}Sr$ and lighter $\delta^{18}O$ than Cottonwood, compatible with increased proportion of arriving Colorado River water. (4) Lake Havasu basin carbonates have $\delta^{13}C$ and $\delta^{18}O$ values similar to values produced by Hualapai waters mixing with Colorado River waters. (5) Bristol basin is more radiogenic in $^{87}Sr/^{86}Sr$ than any of the Bouse basins and was likely hydrochemically distinct and/or poorly mixed with the remainder of Blythe basin. (6) Carbonates of the southern Blythe basin have heavier $\delta^{18}O$ and lighter $\delta^{13}C$ than other Bouse basins and a stable isotope covariation trend similar to that of the modern San Francisco Bay marine estuary. This is compatible with either continued downstream evaporative modification of Bouse waters, and/or intermittent mixing with marine water. The $^{87}Sr/^{86}Sr$ ratios in Bouse carbonates and shells in all basins are more radiogenic than marine values; hence, Bouse carbonate chemistry is distinctly nonmarine. Bouse carbonates have higher $^{87}Sr/^{86}Sr$ than the modern or the 10 ka Colorado River water that fed Lake Cahuilla. Each basin shows different $\delta^{13}C$ and $\delta^{18}O$ mixing trends and a different range of $^{87}Sr/^{86}Sr$ values relative to other basins. This variability suggests different proportions of mixing among Colorado River water, Hualapai basin water, local spring input, and local meteoric input in hydrologically distinct subbasins, in contrast to patterns expected for well-mixed lakes. The only Bouse paleobasin with possible intermittent marine mixing (based on $^{87}Sr/^{86}Sr$, and $\delta^{13}C$

and $\delta^{18}O$ mixing trends, sedimentology, and paleontology) is the southernmost Blythe basin.

Sr mixing models ($^{87}Sr/^{86}Sr$ vs. [Sr]) can explain the wide range in composition of western Colorado Plateau waters by variable mixing of different end-member waters. Model curves yield mixing proportions needed to explain the observed $^{87}Sr/^{86}Sr$ and [Sr] values in various parts of the system. Early Hualapai limestone values (e.g., 0.719) are best explained as being sourced from western Colorado Plateau groundwater. Younger Hualapai values (0.712) can be modeled by a groundwater delivery system adding ~70%–95% higher-elevation Colorado Plateau groundwater similar in composition to Havasu spring groundwater (0.712). This gradual change is recorded in ~50 m of carbonate deposition (1–2 Ma) and hence is unlikely to be a result of arrival of the Colorado River.

Bouse limestone is modeled by mixing first-arriving Colorado River water with late Hualapai (upper 50 m) lake basin water (0.715). Bouse basins show a downstream decrease in maximum $^{87}Sr/^{86}Sr$ values and progressively lighter $\delta^{18}O$ values, both compatible with increasing proportions of Colorado River water relative to initial Hualapai water as the Colorado River became integrated through progressively lower basins. Significant variability of $^{87}Sr/^{86}Sr$ and $\delta^{18}O$ in Bouse basins suggests incomplete mixing during downward integration. The chemistry of Bristol basin carbonates seems to require mixing of radiogenic spring waters (0.713) with local meteoric water or Colorado River water. For the southernmost Blythe basin, where marine fossils and sedimentary structures are present, the moderately elevated Bouse $^{87}Sr/^{86}Sr$ values (0.710–0.712) relative to seawater (0.709) can be explained by adding ~1%–8% endogenic spring/groundwater (e.g., by transport up along faults) to marine water, or by adding ~50% marine water to an average Bouse value of 0.711. We therefore conclude that elevated $^{87}Sr/^{86}Sr$ *cannot* be used to categorically negate the possible influence of marine waters in a marine-estuary environment for the southern Bouse Formation. Nevertheless, our hydrochemical data and modeling generally support a model in which the northern Bouse basins were nonmarine lakes that underwent downward integration due to rapid arrival of Colorado River waters 6–5 Ma. Future work is needed to refine mixing models that include endogenic inputs, surface-water mixing during downward lake basin integration, evolving conditions within each isolated lake system, and the possibility of intermittent mixing with marine waters in the southernmost Blythe basin.

In summary: (1) Hualapai Limestone was deposited by a groundwater system similar to the modern groundwater system such that it records evolving groundwater flow paths on the Colorado Plateau. (2) Increased groundwater input to younger Hualapai basins and groundwater sapping ca. 6–7 Ma may have helped to focus erosion and facilitate integration of the Colorado River through western Grand Canyon at ca. 6 Ma. (3) Grand Wash, Gregg, and Temple basins were hydrochemically and sedimentologically distinct until deposition of uppermost carbonates at ca. 6 Ma; spillover of Grand Wash to Gregg basins is supported by rimstone dams at the spillover point and by the hydrochemistry of $\delta^{13}C$ and $\delta^{18}O$ data, which is compatible with spillover of the combined Grand Wash and Gregg basins to Temple basin ca. 6 Ma. (4) The hydrochemistry of Bouse carbonates can be explained by spillover of Lake Hualapai basin waters that were mixed with early-arriving Colorado River water plus potential groundwater connections. Each Bouse basin has carbonates with distinct hydrochemistry, suggesting incomplete mixing of waters with multiple sources during downward integration of the early Colorado River. Our synthesis highlights the importance of recognizing multiple water sources and mixing scenarios that could have produced the geochemical and isotopic signatures of carbonates in the Hualapai Limestone and Bouse Formation.

ACKNOWLEDGMENTS

This project benefited from partial financial support from National Science Foundation (NSF) grants EAR-0838575 from the Hydrologic Sciences Program, EAR- 1119629, -1242028, and -1348007 from the Tectonics Program, and DGE-0538396 from the NSF GK-12 program. For tephrochronology, Holly Olson performed the laboratory processing and petrography, Dave Wahl conducted the instrumental and computer analysis, and Elmira Wan interpreted the data. Detrital-zircon samples were run by Mark Pecha and the University of Arizona LaserChron laboratory, and we acknowledge NSF grant EAR-1338583 for support of the Arizona LaserChron Center. W.R. Dickinson helped analyze and interpret the detrital-zircon data. Mark Holland created the detrital-zircon figure, and Jason Ricketts helped with drafting of other figures. We thank Viorel Atudori and the University of New Mexico Stable Isotope Laboratory for stable isotope data. The manuscript benefited from discussions and reviews from W.R Dickinson, David Miller, and an anonymous reviewer, as well as from Guest Associate Editor Andres Aslan.

REFERENCES CITED

Albin, A.A., Shastri, L.L., Bowring, S.A., and Karlstrom, K.E., 1991, Geologic and geochronologic data from the Gneiss Canyon shear zone of NW Arizona: Timing and development of orthogonal fabrics: Geological Society of America Abstracts with Programs, v. 23, no. 4, p. 1.

Aslan, A., Karlstrom, K.E., Crossey, L.J., Kelley, S., Cole, R., Lazear, G., and Darling, A., 2010, Late Cenozoic evolution of the Colorado Rockies: Evidence for Neogene uplift and drainage integration, *in* Morgan, L.A., and Quane, S.L., eds., Through the Generations: Geologic and Anthropogenic Field Excursions in the Rocky Mountains from Modern to Ancient: Geological Society of America Field Guide 18, p. 21–54, doi: 10.1130/2010.0018(02).

Augley, J., Huxham, M., Fernandes, T.F., Lyndon, A.R., and Bury, S., 2007, Carbon stable isotopes in estuarine sediments and their utility as migration markers for nursery studies in the Firth of Forth and Forth Estuary, Scotland: Estuarine, Coastal and Shelf Science, v. 72, p. 648–656.

Beard, L.S., 1996, Paleogeography of the Horse Spring Formation in relation to the Lake Mead fault system, Virgin Mountains, Nevada and Arizona, *in* Beratan, K.K., ed., Reconstructing the history of Basin and Range extension using sedimentology and stratigraphy: Boulder, Colorado, Geological Society of America Special Paper 303, p. 27–60.

Beard, L.S., Anderson, R.E., Block, D.L., Bohannon, R.G., Brady, R.J., Castor, S.B., Duebendorfer, E.M., Faulds, J.E., Felger, T.J., Howard, K.A., Kuntz, M.A., and Williams, V.S., 2007, Preliminary Geologic Map of the Lake Mead 30′ x 60′ Quadrangle, Clark County, Nevada, and Mohave County, Arizona: U.S. Geological Survey Open File Report 2007-1010, 109 p.

Billingsley, G.H., Beard, L.S., Priest, S.S., Wellmeyer, J.L., and Block, D.L., 2004, Geologic Map of the Lower Grand Wash Cliffs and Vicinity, Mohave County, Northwestern Arizona: U.S. Geological Survey Miscellaneous Field Studies Map MF-2427.

Blackwelder, E., 1934, Origin of the Colorado River: Geological Society of America Bulletin, v. 45, p. 551–566, doi:10.1130/GSAB-45-551.

Blair, W.N., and Armstrong, A.K., 1979, Hualapai Limestone Member of the Muddy Creek Formation: The Youngest Deposit Predating the Grand Canyon, Southeastern Nevada and Northwestern Arizona: U.S. Geological Survey Professional Paper 1111, 14 p.

Bohannon, R.G., 1984, Nonmarine Sedimentary Rocks of Tertiary Age in the Lake Mead Region, Southeastern Nevada and Northwestern Arizona: U.S. Geological Survey Professional Paper 1259, 72 p.

Buising, A.V., 1988, Depositional and tectonic evolution of the Northern Proto–Gulf of California and Lower Colorado River, as documented in the Mio-Pliocene Bouse Formation and bracketing units, southeastern California and western Arizona [Ph.D. thesis]: Santa Barbara, University of California, 196 p.

Buising, A.V., 1990, The Bouse Formation and bracketing units, southeastern California and western Arizona: Implications for the evolution of the proto–Gulf of California and the lower Colorado River: Journal of Geophysical Research, v. 95, p. 20,111–20,132, doi:10.1029/JB095iB12p20111.

Crossey, L.J., Fischer, T.P., Patchett, P.J., Karlstrom, K.E., Hilton, D.R., Newell, D.L., Huntoon, P., Reynolds, A.C., and de Leeuw, G.A.M., 2006, Dissected hydrologic system at the Grand Canyon: Interaction between deeply derived fluids and plateau aquifer waters in modern springs and travertine: Geology, v. 34, p. 25–28, doi: 10.1130/G22057.1.

Crossey, L.J., Karlstrom, K.E., Springer, A., Newell, D., Hilton, D., and Fischer, T., 2009, Degassing of mantle-derived CO_2 and ^3He from springs in the southern Colorado Plateau region—Flux rates, neotectonics connections, and implications for understanding the groundwater system: Geological Society of America Bulletin, v. 121, no. 7/8, p. 1034–1053, doi:10.1130/B26394.1.

Crossey, L.J., Karlstrom, K.E., Lopez-Pearce, J., and Dorsey, R., 2011, Geochemistry of springs, travertines and lacustrine carbonates of the Grand Canyon region over the past 12 million years: The importance of groundwater on the evolution of the Colorado River system, *in* Beard, L.S., Karlstrom, K.E., Young, R.A., and Billingsley, G.H., eds., CRevolution 2—Origin and Evolution of the Colorado River System, Workshop Abstracts: U.S. Geological Survey Open-File Report 2011–1210, p. 62–67.

Darin, M.H., and Dorsey, R.J., 2013, Reconciling disparate estimates of total offset on the southern San Andreas fault: Geology, v. 41, p. 975–978, doi:10.1130/G34276.1.

Davis, S.J., Mix, H.T., Wiegand, B.A., Carroll, A.R., and Chamberlain, C.P., 2012, Synorogenic evolution of

large-scale drainage patterns: Isotope paleohydrology of sequential Laramide basins: American Journal of Science, v. 309, p. 549–602.

Demeny, A., Kele, S., and Siklosy, Z., 2010, Empirical equations for the temperature dependence of calcite-water oxygen isotope fractionation from 10–70°C: Rapid Communications in Mass Spectrometry, v. 24, p. 3521–3526, doi:10.1002/rcm.4799.

Dickinson, W.R., Lawton, T.F., Pecha, M., Davis, S.J., Gehrels, G.E., and Young, R.A., 2012, Provenance of the Paleogene Colton Formation (Uinta Basin) and Cretaceous–Paleogene provenance evolution in the Utah foreland: Evidence from U-Pb ages of detrital zircons, paleocurrent trends, and sandstone petrofacies: Geosphere, v. 8, p. 854–880, doi:10.1130/GES00763.1.

Dickinson, W.R., Karlstrom, K.E., Grove, M.J., Hanson, A.D., Gehrels, G.E., Pecha, M., Cather, S., Crossey, L.J., Kimbrough, D.L., and Muntean, T.W., 2014, Detrital zircon U-Pb evidence precluding paleo–Colorado River sediment in the exposed Muddy Creek Formation of the Virgin River depression: Geosphere, v. 10, p. 1123–1138, doi:10.1130/GES01097.1.

Doe, B.R., Hedge, C.E., and White, D.E., 1966, Preliminary investigation of the source of lead and strontium in deep geothermal brines underlying the Salton Sea geothermal area: Economic Geology and the Bulletin of the Society of Economic Geologists, v. 61, p. 462–483, doi:10.2113/gsecongeo.61.3.462.

Dorsey, R.J., 2012, Earliest delivery of sediment from the Colorado River to the Salton Trough at 5.3 Ma: Evidence from Split Mountain Gorge, *in* Reynolds, R.E., ed., Searching for the Pliocene: Southern Exposures: Proceedings of the 2012 Desert Symposium, p. 88–93.

Dorsey, R.J., Fluette, A., McDougall, K., Housen, B.A., Janecke, S.U., Axen, G.J., and Shirvell, C.R., 2007, Chronology of Miocene–Pliocene deposits at Split Mountain Gorge, southern California: A record of regional tectonics and Colorado River evolution: Geology, v. 35, p. 57–60, doi:10.1130/G23139A.1.

Dorsey, R.J., Housen, B.A., Janecke, S.U., Fanning, C.M., and Spears, A.L.F., 2011, Stratigraphic record of basin development within the San Andreas fault system: Late Cenozoic Fish Creek–Vallecito basin, southern California: Geological Society of America Bulletin, v. 123, p. 771–793, doi:10.1130/B30168.1.

Eberly, L.D., and Stanley, T.B., Jr., 1978, Cenozoic stratigraphy and geologic history of southwestern Arizona: Geological Society of America Bulletin, v. 89, p. 921–940, doi:10.1130/0016-7606(1978)89<921:CSAGHO>2.0.CO;2.

Faulds, J.E., Wallace, M.A., Gonzales, L.A., and Heizler, M.T., 2001, Depositional environment and paleogeographic implications of the late Miocene Hualapai Limestone, northwestern Arizona and southern Nevada, *in* Young, R.A., and Spamer, E.E., eds., Colorado River: Origin and Evolution: Grand Canyon, Arizona, Grand Canyon Association Monograph 12, p. 81–88.

Felger, T.J., and Beard, L.S., 2010, Geologic map of the Lake Mead and surrounding regions, southern Nevada, southwestern Utah, and northwestern Arizona, *in* Umhoefer, P.J., Beard, L.S., and Lamb, M.A., eds., Miocene Tectonics of the Lake Mead Region, Central Basin and Range: Geological Society of America Special Paper 463, p. 29–38, doi:10.1130/2010.2463(02).

Flowers, R.M., and Farley, K.A., 2012, Apatite ^{4}He/^{3}He and (U-Th)/He evidence for an ancient Grand Canyon: Science, v. 338, p. 1616–1619.

Flowers, R.M., and Farley, K.A., 2013, Response to comments on "Apatite ^{4}He/^{3}He and (U-Th)/He evidence for an ancient Grand Canyon": Science, v. 340, p. 143, doi:10.1126/science.1234203.

Gehrels, G.E., and Pecha, M., 2014, Detrital zircon U-Pb geochronology and Hf isotope geochemistry of Paleozoic and Triassic passive margin strata of western North America: Geosphere, v. 10, no. 1, p. 49–65, doi:10.1130/GES00889.1.

Gehrels, G.E., Valencia, V., and Ruiz, J., 2008, Enhanced precision, accuracy, efficiency, and spatial resolution of U-Pb ages by laser ablation–multicollector–inductively coupled plasma–mass spectrometry: Geochemistry Geophysics Geosystems, v. 9, Q03017, doi:10.1029/2007GC001805.

Gehrels, G.E., Blakey, R., Karlstrom, K.E., Timmons, J.M., Dickinson, B., and Pecha, M., 2011, Detrital zircon U-Pb geochronology of Paleozoic strata in the Grand Canyon, Arizona: Lithosphere, v. 3, p. 183–200, doi:10.1130/L121.1.

Gross, E.L., Patchett, P.J., Dallegge, T.A., and Spencer, J.E., 2001, The Colorado River system and Neogene sedimentary formations along its course: Apparent Sr isotopic connections: Journal of Geology, v. 109, p. 449–461, doi:10.1086/320793.

Hart, W.S., Quade, J., Madsen, D.B., Kaufman, D.S., and Oviatt, C.G., 2004, The ^{87}Sr/^{86}Sr ratios of lacustrine carbonates and lake-level history of the Bonneville paleolake system: Geological Society of America Bulletin, v. 116, p. 1107–1119, doi:10.1130/B25330.1.

Harvey, J., 2014, Zircon age and oxygen isotopic correlations between Bouse Formation tephra and the 4.83 Ma Lawlor Tuff: Geosphere, v. 10, p. 221–232, doi:10.1130/GES0904.1.

Hereford, R., Beard, L.S., Dickinson, W.R., Karlstrom, K.E., Crossey, L.J., Amoroso, L., House, P.K., Heizler, M.T., and Pecha, M., 2015, The late Neogene White Mesa–Crooked Ridge Paleovalley, northeast Arizona—Its age, origin, and relation to carving of Grand Canyon: Geosphere, v. 11, doi:10.1130/GES01124.1 (in press).

Hill, C.A., and Polyak, V.J., 2010, Karst hydrology of Grand Canyon, Arizona, USA: Journal of Hydrology (Amsterdam), v. 390, p. 169–181, doi:10.1016/j.jhydrol.2010.06.040.

Hill, C.A., Eberz, N., and Buecher, R.H., 2008, A karst connection model for Grand Canyon, Arizona, USA: Geomorphology, v. 95, p. 316–334, doi:10.1016/j.geomorph.2007.06.009.

Hill C.A., and Polyak, V.J., 2014, Karst piracy: A mechanism for integrating the Colorado River across the Kaibab uplift, Grand Canyon, Arizona, USA: Geosphere, v. 10, p. 627–640, doi:10.1130/GES00940.1.

Homan, M.B., and Dorsey, R.J., 2013, Sedimentology and stratigraphy of the southern Miocene–Pliocene Bouse Formation: Geological Society of America Abstracts with Programs, v. 45, no. 7, p. 607.

House, P.K., Pearthree, P.A., Howard, K.A., Bell, J.W., Perkins, M.E., Faulds, J.E., and Brock, A.L., 2005, Birth of the lower Colorado River—Stratigraphic and geomorphic evidence for its inception near the conjunction of Nevada, Arizona, and California, *in* Pederson, J.L., and Dehler, C.M., eds., Interior Western United States: Geological Society of America Field Guide 6, p. 357–387.

House, P.K., Pearthree, P.A., and Perkins, M.E., 2008, Stratigraphic evidence for the role of lake spillover in the inception of the lower Colorado River in southern Nevada and western Arizona, *in* Reheis, M.C., Hershler, R., and Miller, D.M., eds., Late Cenozoic Drainage History of the Southwestern Great Basin and Lower Colorado River Region: Geologic and Biotic Perspectives: Geological Society of America Special Paper 439, p. 335–353.

Hunt, C.B., 1956, Cenozoic Geology of the Colorado Plateau: U.S. Geological Survey Professional Paper 279, 99 p.

Hunt, C.B., 1969, Geologic history of the Colorado River, *in* The Colorado River Region and John Wesley Powell: U.S. Geological Survey Professional Paper 669-C, p. 59–130.

Ingram, B.L., and DePaolo, D.J., 1993, A 4300 year strontium isotope record of estuarine paleosalinity in San Francisco Bay, California: Earth and Planetary Science Letters, v. 119, p. 103–119, doi:10.1016/0012-821X(93)90009-X.

Ingram, B.L., and Sloan, D., 1992, Strontium isotopic composition in estuarine and marine sediments as paleosalinity and paleoclimate indicator: Science, v. 255, p. 68–72, doi:10.1126/science.255.5040.68.

Ingram, B.L., Ingle, J.C., and Conrad, M.E., 1996, A 2000 yr record of Sacramento–San Joaquin river inflow to San Francisco Bay estuary: California Geology, v. 24, p. 331–334, doi:10.1130/0091-7613(1996)024<0331:AYROSS>2.3.CO;2.

Karlstrom, K.E., Crow, R., McIntosh, W., Peters, L., Pederson, J., Raucci, J., Crossey, L.J., Umhoefer, P., and Dunbar, N., 2007, ^{40}Ar/^{39}Ar and field studies of Quaternary basalts in Grand Canyon and model for carving Grand Canyon: Quantifying the interaction of river incision and normal faulting across the western edge of the Colorado Plateau: Geological Society of America Bulletin, v. 119, p. 1283–1312, doi:10.1130/0016-7606(2007)119[1283:AAFSOQ]2.0.CO;2.

Karlstrom, K.E., Crow, R, Crossey, L.J., Coblentz, D., and van Wijk, J., 2008, Model for tectonically driven incision of the less than 6 Ma Grand Canyon: Geology, v. 36, no. 11, p. 835–838, 36, doi:10.1130/G25032A.1, with Data Repository 2008218.

Karlstrom, K.E., Lee, J., Kelley, S.A., Crow, R., Young, R.A., Lucchitta, I., Beard, L.S., Dorsey, R., Ricketts, J.W., Dickinson, W.R., and Crossey, L.C., 2013, Arguments for a young Grand Canyon: Technical comment on "R.M. Flowers & K.A. Farley, Apatite ^{4}He/^{3}He and (U-Th)/He evidence for an ancient Grand Canyon": Science, Nov. 2012, doi:10.1126/science.1229390.

Karlstrom, K.E., Lee, J., Kelley, S., Crow, R., Crossey, L., Young, D., Beard, L.S., Ricketts, J., Fox, M., and Shuster, D., 2014, Formation of the Grand Canyon 5 to 6 million years ago through integration of older palaeocanyons: Nature Geoscience, v. 7, p. 239–244, doi:10.1038/ngeo2065.

Kimbrough, D.L., Grove, M., Gehrels, G., Mahoney, J.B., Dorsey, K.A., Howard, K., House, K., Pearthree, P.A., and Flessa, K., 2011, Detrital zircon record of Colorado River integration into the Salton Trough, *in* Beard, L.S., Karlstrom, K.E., Young, R.A., and Billingsley, G.H., eds., CRevolution 2—Origin and Evolution of the Colorado River System, Workshop Abstracts: U.S. Geological Survey Open-File Report 2011–1210, p. 168.

Kimbrough, D.L., Grove, M., Gehrels, G.E., Dorsey, R.J., Howard, K.A., Lovera, O., Aslan, A., House, P.K., and Pearthree, P.A., 2015, Detrital zircon U-Pb provenance record of the Colorado River: Implications for late Cenozoic drainage evolution of the American Southwest: Geosphere, v. 11, doi:10.1130/GES00982.1 (in press).

Lamb, M., Beard, L.S., Foster, M., Dunbar, N., Hickson, T., Umhoefer, P., McIntosh, B., and Karlstrom, K.E., 2015, New provenance data from the Miocene Horse Spring Formation: Evidence for regional uplift in the Lake Mead area, 18–19 Ma, and implications for regional paleodrainage systems: Geosphere, v. 11, doi:10.1130/GES01127.1 (in press).

Lee J.P., Stockli, D.F., Kelley, S.A., Pederson, J.L., Karlstrom, K.E., and Ehlers, T.A., 2013, New Thermochronometric Constraints on the Tertiary Landscape Evolution of Central and Eastern Grand Canyon, Arizona: Geosphere, v. 9, p. 216–228, doi:10.1130/GES00842.1.

Li, H.C., Xu, X.M., Ku, T.L., You, C.F., Buchheim, H.P., and Peters, R., 2008a, Isotopic and geochemical evidence of palaeoclimate changes in Salton Basin, California, during the past 20 kyr: 1. δ^{18}O and δ^{13}C records in lake tufa deposits: Palaeogeography, Palaeoclimatology, Palaeoecology, v. 259, p. 182–197, doi:10.1016/j.palaeo.2007.10.006.

Li, H.C., You, C.F., Ku, T.L., Xu, X.M., Buchheim, H.P., Wan, N.J., Wang, R.M., and Shen, M.L., 2008b, Isotopic and geochemical evidence of palaeoclimate changes in Salton Basin, California, during the past 20 kyr: 2. ^{87}Sr/^{86}Sr ratio in lake tufa as an indicator of connection between Colorado River and Salton Basin: Palaeogeography, Palaeoclimatology, Palaeoecology, v. 259, p. 198–212, doi:10.1016/j.palaeo.2007.10.007.

Lucchitta, I., 1966, Cenozoic Geology of the Lake Mead Area Adjacent to the Grand Wash Cliffs, Arizona [Ph.D. dissertation]: The Pennsylvania State University, 218 p.

Lucchitta, I., 1972, Early history of the Colorado River in the Basin and Range Province: Geological Society of America Bulletin, v. 83, p. 1933–1948, doi:10.1130/0016-7606(1972)83[1933:EHOTCR]2.0.CO;2.

Lucchitta, I., 1979, Late Cenozoic uplift of the southwestern Colorado Plateau and adjacent LCR region: Tectonophysics, v. 61, p. 63–95, doi:10.1016/0040-1951(79)90292-0.

Lucchitta, I., 2013, Comment on "Apatite ^{4}He-^{3}He and (U-Th)/He evidence for an ancient Grand Canyon": Science, v. 340, p. 143, doi:10.1126/science.1234567.

Ludwig, K.R., 1993, A Computer Program for Processing Pb-U-Th Isotope Data: U.S. Geological Survey Open-File Report 88–542, 33 p.

Ludwig, K.R., 2001, User's Manual for Isoplot/Ex Version 2.2: Berkeley Geochronology Center Special Publication 1a, 53 p.

McDougall, K., 2008, Late Neogene marine incursions and the ancestral Gulf of California, *in* Reheis, M.C., Hershler, R., and Miller, D.M., eds., Late Cenozoic Drainage History of the Southwestern Great Basin and Lower Colorado River Region: Geologic and Biotic Perspectives: Geological Society of America Special Paper 439, p. 355–373.

McDougall, K., 2010, Update on Microfossil Studies in the Northern Gulf of California, Salton Trough and Lower Colorado River, *in* Beard, L.S., et al., eds., CRevolution 2—Origin and evolution of the Colorado River system, workshop abstracts: U.S. Geological Survey Open-File Report 2011–1210, p. 218–221.

McDougall, K., and Miranda Martinez, A.Y., 2014, Evidence for a marine incursion along the lower Colorado River: Geosphere, v. 10, p. 842–869, doi:10.1130/GES00975.1.

Metzger, D.G., 1968, The Bouse Formation (Pliocene) of the Parker-Blythe-Cibola Area, Arizona and California: U.S. Geological Survey Professional Paper 600-D, p. D126–D136.

Metzger, D.G., Loeltz, O.J., and Irelan, B., 1973, Geohydrology of the Parker-Blythe-Cibola Area, Arizona and California: U.S. Geological Survey Professional Paper 486-G, 130 p.

Miller, D.M., Reynolds, R.E., Bright, J.E., and Starratt, S.W., 2014, Bouse Formation in the Bristol basin near Amboy, California: Geosphere, v. 10, no. 3, p. 462–475, doi:10.1130/GES00934.1.

O'Brien, G.R., 2002, Oxygen Isotope Composition of Banded Quaternary Travertine, Grand Canyon National Park, Arizona [M.S. thesis]: Flagstaff, Arizona, Department of Geology. Northern Arizona University, 80 p.

O'Brien, G.R., Kaufman, D.S., Sharp, W.D., Atudorei, V., Parnell, R.A., and Crossey, L.J., 2006, Oxygen isotope composition of annually banded modern and mid-Holocene travertine and evidence of paleomonsoon floods, Grand Canyon, Arizona, USA: Quaternary Research, v. 65, p. 366–379, doi:10.1016/j.yqres.2005.12.001.

Olmsted, F.H., Loeltz, O.J., and Irelan, B., 1973, Geohydrology of the Yuma area, Arizona and California: Water resources of lower Colorado River-Salton Sea area. U.S. Geological Survey Professional Paper 486-H, 227 p.

Oskin, M., and Stock, J., 2003, Pacific–North America plate motion and opening of the Upper Delfin Basin, northern Gulf of California, Mexico: Geological Society of America Bulletin, v. 115, p. 1173–1190, doi:10.1130/B25154.1.

Patchett, P.J., and Spencer, J., 2001, Application of Sr isotopes to hydrology of Colorado system waters and potentially related Neogene sedimentary formations, *in* Young, R.A., and Spamer, E.E., eds., The Colorado River: Origin and Evolution: Grand Canyon, Arizona, Grand Canyon Association Monograph 12, p. 167–171.

Pearce, J.L., 2010, Syntectonic Deposition and Paleohydrology of the Spring-Fed Hualapai Limestone and Implications for 5–6 Ma Integration of the Colorado River System Through Grand Canyon: Evidence from Sedimentology, Chemostratigraphy and Detrital Zircon Analysis [M.S. thesis]: Albuquerque, New Mexico, University of New Mexico, 205 p.

Pearce, J.L., Crossey, L.J., Karlstrom, K.E., Gehrels, G., Pecha, M., Beard, L.S., and Wan, E., 2011 Syntectonic deposition and paleohydrology of the spring-fed Hualapai Limestone and implications for the 6–5 Ma integration of the Colorado River system through the Grand Canyon, *in* Beard, L.S., Karlstrom, K.E., Young, R.A., and Billingsley, G.H., eds., CRevolution 2—Origin and Evolution of the Colorado River System, Workshop Abstracts: U.S. Geological Survey Open-File Report 2011–1210, p. 180–185.

Pearthree, P.A., and House, P.K., 2014, Paleogeomorphology and evolution of the early Colorado River inferred from relationships in Mohave and Cottonwood valleys, Arizona, California, and Nevada: Geosphere, v. 10, p. 1139–1160, doi:10.1130/GES00988.1.

Pederson, D.T., 2001, Stream piracy revisited: A ground water sapping solution: GSA Today, v. 11, no. 9, p. 4–10, doi:10.1130/1052-5173(2001)011<0004:SPRAGS>2.0.CO;2.

Pederson, J., 2008, The mystery of the pre–Grand Canyon Colorado River—Results from the Muddy Creek Formation: GSA Today, v. 18, no. 3, p. 4–10, doi:10.1130/GSAT01803A.1.

Pederson, J., Karlstrom, K.E., McIntosh, W.C., and Sharp, W., 2002, Geomorphic implications of new absolute ages and associated incision and fault-slip rates in Grand Canyon: Geology, v. 30, no. 8, p. 739–742.

Plattner, C., Malservisi, R., Dixon, T.H., LaFemina, P., Sella, G.F., Fletcher, J., and Suarez-Vidal, F., 2007, New constraints on relative motion between the Pacific plate and Baja California microplate (Mexico) from GPS measurements: Geophysical Journal International, v. 170, p. 1373–1380, doi:10.1111/j.1365-246X.2007.03494.x.

Polyak, V., Hill, C., and Asmerom, Y., 2008, Age and evolution of the Grand Canyon revealed by U-Pb dating of water table–type speleothems: Science, v. 319, p. 1377–1380, doi:10.1126/science.1151248.

Poulson, S.R., and John, B.E., 2003, Stable isotope and trace element geochemistry of the basal Bouse Formation carbonate, southwestern United States: Implications for the Pliocene uplift history of the Colorado Plateau: Geological Society of America Bulletin, v. 115, p. 434–444, doi:10.1130/0016-7606(2003)115<0434:SIATEG>2.0.CO;2.

Romanek, C.S., Grossman, E.L., and Morse, J.W., 1992, Carbon isotopic fractionation in synthetic aragonite and calcite: Effects of temperature and precipitation rate: Geochimica et Cosmochimica Acta, v. 56, p. 419–430.

Roskowski, J.A., Patchett, P.J., Spencer, J.E., Pearthree, P.A., Dettman, D.L., Faulds, J.E., and Reynolds, A.C., 2010, A late Miocene–early Pliocene chain of lakes fed by the Colorado River: Evidence from Sr, C, and O isotopes of the Bouse Formation and related units between Grand Canyon and the Gulf of California: Geological Society of America Bulletin, v. 122, p. 1625–1636, doi:10.1130/B30186.1.

Sampei, Y., Matsumoto, E., Dettman, D.L., Tokuoka, T., and Abe, O., 2005, Paleosalinity in a brackish lake during the Holocene based on stable oxygen and carbon isotopes of shell carbonate in Nakaumi Lagoon, southwest Japan: Palaeogeography, Palaeoclimatology, Palaeoecology, v. 224, p. 352–366.

Scarborough, R., 2001, Neogene development of the Little Colorado River Valley and eastern Grand Canyon: Field evidence for an overtopping hypothesis, *in* Young, R.A., and Spamer, E.E., eds., The Colorado River: Origin and Evolution: Grand Canyon, Arizona, Grand Canyon Association Monograph 12, p. 207–212.

Seixas, G., Resor, P., Pearce, J.L., Karlstrom, K., and Crossey, L., 2015, Constraints on the evolution of vertical deformation and Colorado River incision near eastern Lake Mead, Arizona, provided by quantitative structural mapping of the Hualapai Limestone: Geosphere, v. 11, p. 31–49, doi:10.1130/GES01096.1.

Sharp, Z., 2007, Principles of Stable Isotope Geochemistry: Upper Saddle River, New Jersey, Pearson Education, Inc., 360 p.

Smith, P.B., 1970, New evidence for a Pliocene marine embayment along the lower Colorado River area, California and Arizona: Geological Society of America Bulletin, v. 81, p. 1411–1420.

Spencer, J.E., and Patchett, P.J., 1997, Sr isotope evidence for a lacustrine origin for the upper Miocene to Pliocene Bouse Formation, lower Colorado River trough, and implications for timing of Colorado Plateau uplift: Geological Society of America Bulletin, v. 109, p. 767–778, doi:10.1130/0016-7606(1997)109_0767:SIEFAL_2.3.CO;2.

Spencer, J.E., Peters, L., McIntosh, W.C., and Patchett, P.J., 2001, $^{40}Ar/^{39}Ar$ geochronology of the Hualapai Limestone and Bouse Formation and implications for the age of the lower Colorado River, *in* Young, R.A., and Spamer, E.E., eds., The Colorado River: Origin and Evolution: Grand Canyon, Arizona, Grand Canyon Association Monograph 12, p. 89–91.

Spencer, J.E., Pearthree, P.A., and House, P.K., 2008, An evaluation of the evolution of the latest Miocene to earliest Pliocene Bouse lake system in the lower Colorado River valley, southwestern USA, *in* Reheis, M.C., Hershler, R., and Miller, D.M., eds., Late Cenozoic Drainage History of the Southwestern Great Basin and Lower Colorado River Region: Geologic and Biotic Perspectives: Geological Society of America Special Paper 439, p. 373–388, doi:10.1130/2008.2439(17).

Spencer, J.E., Patchett, P.J., Pearthree, P.A., House, P.K., Sarna-Wojcicki, A.M., Wan, E., Roskowski, J.A., and Faulds, J.E., 2013, Review and analysis of the age and origin of the Pliocene Bouse Formation, lower Colorado River Valley, southwestern USA: Geosphere, v. 9, no. 3, p. 444–459, doi:10.1130/GES00896.1.

Spötl, C., and Venneman, T., 2003, Continuous-flow isotope ratio mass spectrometric analysis of carbonate minerals: Rapid Communications in Mass Spectrometry, v. 17, doi:10.1002/rcm.1010.

Talbot, M.R., 1990, A review of the paleohydrological interpretation of carbon and oxygen isotopic ratios in primary lacustrine carbonates: Chemical Geology–Isotope Geoscience Section, v. 80, p. 261–279, doi:10.1016/0168-9622(90)90009-2.

Talbot, M.R., 1994, Paleohydrology of the late Miocene Ridge basin lake, California: Geological Society of America Bulletin, v. 106, no. 9, p. 1121–1129, doi:10.1130/0016-7606(1994)106<1121:POTLMR>2.3.CO;2.

Talbot, M.R., and Kelts, K., 1990, Paleolimnological signatures from carbon and oxygen isotopic ratios in carbonates from organic carbon–rich lacustrine sediments, *in* Katz, B., ed., Lacustrine Basin Exploration: Case Studies and Modern Analogs: American Association of Petroleum Geologists Memoir 50, p. 99–112.

Wallace, M.A., Faulds, J.E., and Brady, R.J., 2005, Geologic Map of the Meadview North Quadrangle, Mohave County, Arizona, and Clark County, Nevada: Nevada Bureau of Mines and Geology Map 154, scale 1:24,000, 1 sheet.

Wernicke, B., 2011, The California River and its role in carving Grand Canyon: Geological Society of America Bulletin, v. 123, p. 1288–1316, doi:10.1130/B30274.1.

Young, R.A., 2008, Pre–Colorado River drainage in western Grand Canyon: Potential influence on Miocene stratigraphy in Grand Wash Trough, *in* Reheis, M.C., Hershler, R., and Miller, D.M., eds., Late Cenozoic Drainage History of the Southwestern Great Basin and Lower Colorado River Basin: Geologic and Biotic Perspectives: Geological Society of America Special Paper 439, p. 319–333.

Geosphere

Importance of groundwater in propagating downward integration of the 6–5 Ma Colorado River system: Geochemistry of springs, travertines, and lacustrine carbonates of the Grand Canyon region over the past 12 Ma

L.C. Crossey, K.E. Karlstrom, R. Dorsey, J. Pearce, E. Wan, L.S. Beard, Y. Asmerom, V. Polyak, R.S. Crow, A. Cohen, J. Bright and M.E. Pecha

Geosphere 2015;11;660-682
doi: 10.1130/GES01073.1

Notes